agronomy

MDPI

Article

Assessing the Impact of Multi-Decadal Land Use Change on Agricultural Water–Energy Dynamics in the Awash Basin, Ethiopia: Insights from Remote Sensing and Hydrological Modeling

Tewekel Melese Gemechu [1,2,3], Huifang Zhang [1], Jialong Sun [4,5,6,*] and Baozhang Chen [1,2,4,7,*]

[1] State Key Laboratory of Resource and Environmental Information System, Institute of Geographic Sciences and Natural Resources Research, Chinese Academy of Sciences, Beijing 100101, China; tmgemechu2022@igsnrr.ac.cn (T.M.G.); zhanghf@lreis.ac.cn (H.Z.)
[2] University of Chinese Academy of Sciences, No. 19A, Yuquan Road, Beijing 100049, China
[3] Department of Natural Resource Management, Ambo University, Ambo P.O. Box 19, Ethiopia
[4] School of Marine Technology and Surveying, Jiangsu Ocean University, Lianyungang 222001, China
[5] Jiangsu Key Laboratory of Marine Meteorology Disaster Prevention and Mitigation, Lianyungang 222001, China
[6] Jiangsu Marine Remote Sensing Engineering Research Center, Lianyungang 222001, China
[7] School of Environmental Science and Engineering, Nanjing University of Information Science and Technology, Nanjing 210044, China
* Correspondence: 2006000076@jou.edu.cn (J.S.); baozhang.chen@igsnrr.ac.cn (B.C.)

Abstract

Sustainable agriculture in semi-arid regions like the Awash Basin is critically dependent on water availability, which is increasingly threatened by rapid land use and land cover (LULC) change. This study assesses the impact of multi-decadal LULC changes on water resources essential for agriculture. Using satellite-derived LULC scenarios (2001, 2010, 2020) to drive the WRF-Hydro/Noah-MP modeling framework, we provide a holistic assessment of water dynamics in Ethiopia's Awash Basin. The model was calibrated and validated with observed streamflow (R^2 = 0.80–0.89). Markov analysis revealed rapid cropland expansion and urbanization (2001–2010), followed by notable woodland recovery (2010–2020) linked to national initiatives. Simulations show that early-period changes increased surface runoff, potentially enhancing reservoir storage for large-scale irrigation. In contrast, later changes promoted subsurface flow, indicating a shift towards enhanced groundwater recharge, which is critical for small-scale and well-based irrigation. Evapotranspiration (ET) trends, validated against GLEAM (monthly R^2 = 0.88–0.96), reflected these shifts, with urbanization suppressing water fluxes and woodland recovery fostering their resurgence. This research demonstrates that land use trajectories directly alter the partitioning of agricultural water sources. The findings provide critical evidence for designing sustainable land and water management strategies that balance crop production with forest conservation to secure irrigation water and support initiatives like Ethiopia's Green Legacy Initiative.

Keywords: agricultural water management; irrigation; land use change; evapotranspiration; surface runoff; subsurface flow; soil moisture; Awash Basin; Ethiopia

check for updates

Academic Editor: Gianni Bellocchi

Received: 30 October 2025
Revised: 28 November 2025
Accepted: 28 November 2025
Published: 5 December 2025

Citation: Gemechu, T.M.; Zhang, H.; Sun, J.; Chen, B. Assessing the Impact of Multi-Decadal Land Use Change on Agricultural Water–Energy Dynamics in the Awash Basin, Ethiopia: Insights from Remote Sensing and Hydrological Modeling. *Agronomy* **2025**, *15*, 2804. https://doi.org/10.3390/agronomy15122804

Copyright: © 2025 by the authors. Licensee MDPI, Basel, Switzerland. This article is an open access article distributed under the terms and conditions of the Creative Commons Attribution (CC BY) license (https://creativecommons.org/licenses/by/4.0/).

1. Introduction

Water is a fundamental input for agricultural production, critically governing food security and economic development in arid and semi-arid regions [1]. In these vulnerable areas,

land use and land cover (LULC) change, particularly the conversion of natural ecosystems to cultivated land, is a significant human-induced force that profoundly alters the hydrological cycle, impacting the availability of water for irrigation [2]. Satellite-based analyses reveal that agricultural expansion is a dominant driver of environmental change in Ethiopia, directly affecting the water balance upon which rain-fed and irrigated agriculture depend [3]. Understanding these dynamics is essential for sustainable agricultural water management, a challenge acutely felt in Ethiopia's Awash Basin, a vital semi-arid region and a cornerstone of the nation's agriculture, facing escalating threats from water scarcity and climate change [4,5].

The Awash Basin, a cornerstone of Ethiopia's agriculture and hydroelectric power, exhibits significant hydrological complexity due to its diverse terrain, seasonal rainfall patterns, and intense human pressure [6]. The basin supports extensive irrigated agriculture for cash crops like sugarcane and cotton, as well as staple crops, making the sustainability of its water resources a national priority [7]. Research in the basin, however, remains fragmented, with most studies focusing on the upper or middle reaches, leaving the lower, more arid areas under-researched [8,9]. This gap limits our understanding of crucial basin-wide processes such as runoff dynamics, soil moisture variability, and groundwater–surface water interactions. Furthermore, the conversion of natural vegetation to cultivated land and urban areas is a dominant driver of environmental change in Ethiopia, significantly impacting the hydrological balance and accelerating soil erosion [3]. These LULC changes, coupled with climate variability, lead to shifts in precipitation patterns and increased frequency of droughts and floods, complicating water resource planning and management [4,10].

The WRF-Hydro/Noah-MP model is a sophisticated tool for simulating hydrological responses to land use and land cover change (LUCC) due to its detailed representation of land-atmosphere interactions and hydrological processes [11,12]. The model's responsiveness to LUCC is attributed to its ability to dynamically integrate changes in land surface characteristics, including vegetation processes, soil moisture-vegetation interactions, and energy partitioning. These elements are directly influenced by land surface parameters such as leaf area index, albedo, and roughness length, which are altered by LUCC, for example, during the conversion of natural vegetation to urban or agricultural land [13]. Such conversions lead to significant shifts in surface energy balance, water infiltration, and runoff patterns [14]. Notably, agricultural expansion and urbanization have increased streamflow in some areas, such as the Kesem Watershed, where agrarian land expansion led to a 23.2% increase in mean annual streamflow between 1993 and 2005 [10]. However, these changes also pose challenges, including increased sedimentation in reservoirs like Koka Dam, which affects water storage and power generation capacity [8].

Evapotranspiration (ET) is a key parameter in this system, representing the main form of energy and water exchange in the soil-vegetation-atmosphere continuum [15]. Accurate estimation of regional ET is crucial for rational water allocation [16], as it accounts for a significant portion of precipitation loss globally [17]. Changes in land use directly affect meteorological parameters that influence ET, such as wind speed and solar radiation [18]. Therefore, quantifying ET dynamics in response to LULC change is critical for managing water resources, irrigation, and developing best management practices.

Integrating remote sensing with advanced ecohydrological models offers a powerful approach to overcome data scarcity and provide comprehensive, spatially explicit assessments of water and energy fluxes [19]. Satellite-based observations and products, such as those from the Global Land Data Assimilation System (GLDAS), enable continuous monitoring of hydrological parameters at large spatial scales, which is essential for capturing the impacts of climate and land cover dynamics [20]. In this context, the coupled WRF-Hydro/Noah-MP model emerges as a robust tool. WRF-Hydro, a distributed hydrological model extension of the Weather Research and Forecasting model, integrates

atmospheric dynamics with surface and subsurface hydrology [21]. Coupled with the Noah-MP land surface model, which includes multiple parameterization options for vegetation and soil processes, this framework can significantly enhance the simulation of water balance components and energy fluxes across complex terrains [22,23].

The basin's hydrological dynamics are further complicated by extreme weather events, such as the severe flooding in 2020, which was exacerbated by heavy rainfall in both the upper and lower basins [24]. Understanding these climate differences and their impacts on water resources is crucial for effectively managing the basin's water supply, especially given the growing demands from agriculture, industry, and urbanization [25].

The Awash Basin faces several hydrological challenges, including water scarcity, variable precipitation, and high evaporation rates. Water scarcity is a significant issue due to over-extraction for agricultural and industrial use, leading to declining water levels in rivers and reservoirs [26]. The variability in precipitation, with erratic and uneven rainfall distribution, exacerbates the problem of water availability [27]. High evaporation rates, particularly in lowland areas, further reduce the available water, impacting both surface and groundwater resources [28]. Additionally, the basin suffers from salinization and declining water quality, resulting from intensive irrigation practices and inadequate drainage systems [29]. These challenges require implementing integrated water resource management strategies to ensure sustainable water use and mitigate the impacts of climate and land use change on the basin's hydrology.

While previous studies have examined the impacts of land use change on hydrology across various regions [3,27,28], a critical gap remains in understanding how decadal land use trajectories specifically affect water sources for agriculture. Few, if any, have dynamically integrated multi-decadal LUC scenarios directly into a fully coupled, process-based model like WRF-Hydro/Noah-MP to attribute changes in water partitioning between surface runoff (for reservoirs) and subsurface flow (for groundwater) to specific land transitions. This is particularly relevant for the Awash Basin, where studies have shown significant LULC-driven changes in streamflow [10] and sediment yield [8], but without a dynamic, process-based attribution of these changes to water availability for cropping systems.

This study introduces a novel framework that bridges this gap by embedding multi-decadal LULC scenarios (2001, 2010, and 2020) directly into the WRF-Hydro/Noah-MP modeling system to assess their impact on water resources critical to agriculture in Ethiopia's Awash Basin from 2001 to 2024. The innovation of this research lies in the dynamic integration of observed decadal land use transitions to isolate the hydrological effects of LULC from interannual climate variability. This approach allows for a temporally explicit analysis of how land use trajectories—such as agricultural expansion, urbanization, and afforestation—interact to shape key variables in agricultural water management, including evapotranspiration (a measure of crop and ecosystem water use), surface runoff, and subsurface flow. The specific objectives of this study are to (1) assess the impact of decadal LULC changes (2001–2020) on hydrologic processes governing irrigation water supply using the coupled WRF-Hydro/Noah-MP model; (2) evaluate the associated trade-offs in water fluxes between different land use trajectories; and (3) derive implications for sustainable agricultural water management and land use policy in the Awash Basin, providing actionable insights for initiatives like Ethiopia's Green Legacy Initiative [30,31].

2. Study Area Description and Methodology

2.1. Description of the Study Area

The Awash Basin, located in the central part of Ethiopia (approximately 8–12° N, 38–43° E), is one of the most significant and critically stressed river basins in the Horn of Africa [4]. At a continental scale, it represents a quintessential example of a semi-arid to

arid river system in East Africa, where water resources are under intense pressure from rapid population growth, agricultural development, and climate variability [32]. As a closed basin with no outlet to the sea, its hydrological dynamics are particularly sensitive to internal changes, making it a critical case for studying land-water interactions. The Awash Basin spans diverse climatic zones, ranging from humid highlands to arid lowlands, covering approximately 110,000 km^2. The basin is critical for agriculture, water supply, and hydroelectric power generation [7]. Characterized by seasonal rainfall variability and prolonged dry periods, the basin faces over-extraction, salinization, and declining water quality challenges. The basin's topography is complex, with elevations ranging from over 4000 m in the highlands to below sea level in the lowlands. This variation in elevation contributes to a wide range of climatic conditions, from temperate conditions in the highlands to hot, dry conditions in the lowlands [6]. The complex topography and diverse land use, including forests, grasslands, and urban areas, further complicate hydrological processes, making it an ideal case study for evaluating advanced coupled models. The basin experiences significant seasonal rainfall variability, with most precipitation occurring during the primary rainy season (Kiremt) from June to September [33]. This variability and prolonged dry periods challenge water resource management and agricultural productivity [25]. The Awash Basin in Ethiopia exhibits a diverse climate, ranging from humid subtropical in the highlands to arid conditions in the lowlands [25]. This variability significantly influences precipitation patterns across the basin. The upper basin receives substantial rainfall, often exceeding 1200 mm annually, with a bimodal distribution: a short rainy season from March to May and the main rains from June to September [24]. In contrast, the lower basin receives much less rainfall, typically below 100 mm per year [24]. Climate change is projected to exacerbate these differences, with models suggesting a decrease in runoff due to warmer, drier conditions, potentially reducing water availability by 10–34% across different scenarios [6].

Nationally, the Awash Basin is a cornerstone of Ethiopia's economy and food security. It encompasses the capital city, Addis Ababa, and supports extensive irrigated agriculture for cash crops (e.g., sugarcane and cotton) and staple foods, contributing substantially to the national GDP. The basin also hosts a cascade of hydroelectric dams, which are vital for the country's energy supply [8]. However, it faces severe challenges, including water scarcity, salinization, and declining water quality, exacerbated by climate change and unsustainable land use practices.

The selection of the Awash Basin for this study is therefore motivated by its (1) national socio-economic importance, (2) representation of diverse hydro-climatic zones (from humid highlands to arid lowlands) within a single basin, (3) documented history of rapid and multifaceted LULC change, including agricultural expansion, urbanization, and recent large-scale afforestation efforts (e.g., the Green Legacy Initiative), and (4) its status as a data-scarce region where advanced modeling approaches are essential for informed water resource management. This combination of factors makes the Awash Basin an ideal and urgent case study for assessing the impacts of decadal land use trajectories on agricultural water resources.

2.2. Remote Sensing Data Acquisition and Processing

2.2.1. Meteorological Forcing Data

We utilized the Global Land Data Assimilation System (GLDAS-2.1) for hydrological modeling in the Awash Basin to provide high-resolution meteorological forcing data at 3 h intervals [20]. GLDAS, developed by NASA, NOAA, and other institutions, integrates data from advanced observing systems to improve forecast initial conditions [20,34]. It drives land surface models such as Noah-MP, Mosaic, CLM, and VIC, simulating the transfer of

mass, energy, and momentum [35]. GLDAS updates these simulations by merging them with satellite and ground-based observations through data assimilation techniques like the Ensemble Kalman Filter and the Extended Kalman Filter [36]. The system runs at various grid resolutions, including 0.25° × 0.25°, with results available near real time [37]. Multiple versions of GLDAS exist, such as GLDAS-2, which uses Princeton meteorological forcing data, and GLDAS-2.1, which combines model- and observation-based data [20]. This study used the WRF-Hydro/NoahMP model with GLDAS meteorological data, including precipitation, shortwave and longwave radiation, air temperature, air pressure, specific humidity, and wind speed.

2.2.2. Land Use/Land Cover (LULC) Data

The remote sensing and model data supporting the findings of this study are openly available. The ESA CCI Land Cover data can be accessed at https://www.esa-landcover-cci.org/?q=node/199 (accessed on 1 February 2025) [38]. The land use/land cover (LUC) scenarios for the years 2001, 2010, and 2020 were derived from the ESA Climate Change Initiative (ESA CCI) Land Cover dataset, a globally harmonized, annually resolved product at 300 m spatial resolution [38]. The ESA CCI dataset is a processed, value-added remote sensing product that integrates observations from multiple sensors and applies consistent classification schemes (based on the UN-LCCS) across years. It was chosen for this study due to its temporal consistency, global availability, and suitability for multi-decadal land change analysis. The selected spatial resolution optimally leverages the detail provided by the 300 m ESA CCI land cover data while maintaining computational efficiency for multi-decadal simulations across the extensive basin.

2.2.3. Validation Using Remote Sensing Products

The GLDAS data were acquired from https://ldas.gsfc.nasa.gov/gldas (Accessed on 20 February 2025). The GLEAM ET data are available at www.gleam.eu. Evapotranspiration (ET) represents the actual water consumption by crops and ecosystems, making it a critical metric for agricultural water management. The WRF-Hydro/NoahMP model's performance was assessed by comparing simulated evapotranspiration (ET) against GLEAM ET data (2003–2022) [39,40] and GLDAS-derived ET data (2000–2024) [20] under three distinct land use scenarios for the Awash Basin: 2001, 2010, and 2020. The ERA5 reanalysis data were downloaded from the Copernicus Climate Data Store https://cds.climate.copernicus.eu (Accessed on 1 June 2025). The streamflow data are available from the corresponding author upon reasonable request due to restrictions (e.g., privacy or ethical concerns).

The performance of the WRF-Hydro/Noah-MP model was rigorously assessed using a multi-source remote sensing validation framework. While observed streamflow data from in situ monitoring stations (Metehara and Adaitu) provided direct hydrological validation, the model's representation of land surface processes was evaluated against independent satellite-based products. Simulated evapotranspiration (ET) was compared against the satellite-based GLEAM ET product (2003–2022), which provides a global benchmark for evaporative fluxes derived primarily from microwave remote sensing. Furthermore, latent heat flux and ET simulations were validated against the Global Land Data Assimilation System (GLDAS, 2000–2024), which assimilates multiple satellite observations into its land surface modeling framework. This tripartite validation approach—using in situ discharge, remote-sensing-based ET, and a satellite-assimilated land-surface product—ensured a robust evaluation of the model's capability to simulate integrated water and energy dynamics.

2.3. Overview of the Methodology

This study integrates multi-decadal land use change (LUC) scenarios (2001, 2010, and 2020) into the WRF-Hydro/Noah-MP modeling framework to simulate water–energy dynamics in Ethiopia's Awash Basin. The integration of these land use scenarios into the model is the primary innovation of this study, as no previous research has dynamically incorporated decadal LUC transitions into such a comprehensive hydrological framework.

2.3.1. WRF-Hydro/Noah-MP Model Overview and Setup

The WRF-Hydro model was developed by the National Center for Atmospheric Research (NCAR) as part of their efforts to improve hydrometeorological and hydrologic modeling [21]. It focuses on simulating the movement and distribution of water in the hydrological cycle, including surface and subsurface flow. The Noah-Multiparameterization (Noah-MP) land surface model is an advanced version of the Noah model that includes multiple parameterizations to represent land surface processes more accurately, including soil moisture, snow, and vegetation dynamics [22].

The Ethiopian basin, which encompasses vital watersheds like the Blue Nile and the Awash River, plays a crucial role in regional water supply, agriculture, and hydropower generation [41,42]. However, the basin faces increasing challenges due to climate variability, land use changes, and population growth. Understanding and accurately simulating components of the water balance, such as runoff, evapotranspiration (ET), groundwater, and surface water storage, is essential for managing these water resources sustainably [43–45]. WRF-Hydro (Weather Research and Forecasting Hydrological extension) is a widely used distributed hydrological model that integrates atmospheric dynamics with surface and subsurface hydrology, enabling the simulation of hydrological processes across scales [46]. Coupling WRF-Hydro with the advanced Noah-MP land surface model (Noah with Multi-Parameterization options) can further enhance these simulations by incorporating multiple parameterization schemes for land surface processes, vegetation, and soil hydrology [23]. In the Ethiopian basin, where complex terrain and diverse climatic conditions prevail, this coupling has the potential to significantly improve the accuracy of water balance simulations.

2.3.2. Model Grid Domain and Physics Parameterizations

This study configured the WRF-Hydro/Noah-MP model to account for key land-atmosphere processes using specific parameterization options [47]. Dynamic vegetation (DVEG) was activated, allowing the model to use look-up table values for LAI and the maximum vegetation fraction, thereby enabling a realistic representation of seasonal vegetation dynamics. The Ball-Berry scheme was selected for canopy stomatal resistance (OPT_CRS), allowing stomatal conductance to respond to environmental drivers such as humidity and CO_2 concentration [48]. To model the effect of soil moisture on stomatal resistance, the Noah-based approach (OPT_BTR) was applied [21]. Runoff and groundwater processes (OPT_RUN) were simulated using the TOPMODEL-based method with groundwater interaction, allowing saturation-excess runoff and lateral subsurface flow [49]. Surface resistance to evaporation and sublimation (OPT_RSF) was parameterized following Sakaguchi and Zeng (2009) [50], which better represents resistance under varying surface wetness and vegetation cover. Lastly, soil hydraulic and thermal properties (OPT_SOIL) were assigned based on dominant soil texture classes from the input datasets, ensuring spatial consistency in infiltration and soil moisture behavior across the basin. Other physics options typically employed include land-surface parameterizations, such as the Noah-MP model, which accounts for overland surface flow, saturated subsurface flow, and channel routing [51].

For simulations in the Awash Basin, the model domain is typically set to cover the entire basin, approximately 110,000 km^2 (Figure 1). The spatial resolution used in these

models can vary, but a common choice is a routing grid size of 600 m and a domain grid size of 6 km × 6 km to capture detailed topography and land use variations [52]. To ensure consistency within the WRF-Hydro/Noah-MP modeling framework, all datasets were processed to the model's domain grid. The GLDAS meteorological forcing data (0.25° native resolution) were interpolated to the 6 km WRF-Hydro grid using the Earth System Modeling Framework (ESMF) with a bilinear interpolation method, as implemented in an NCL script. For the land surface representation, the high-resolution ESA CCI land cover data and other static geographical fields were processed through the WRF Preprocessing System (WPS) using the geogrid.exe program. This system utilizes the default WRF geographical datasets to generate the model's static fields, including topography and land use categories, at the specified 6 km domain grid resolution.

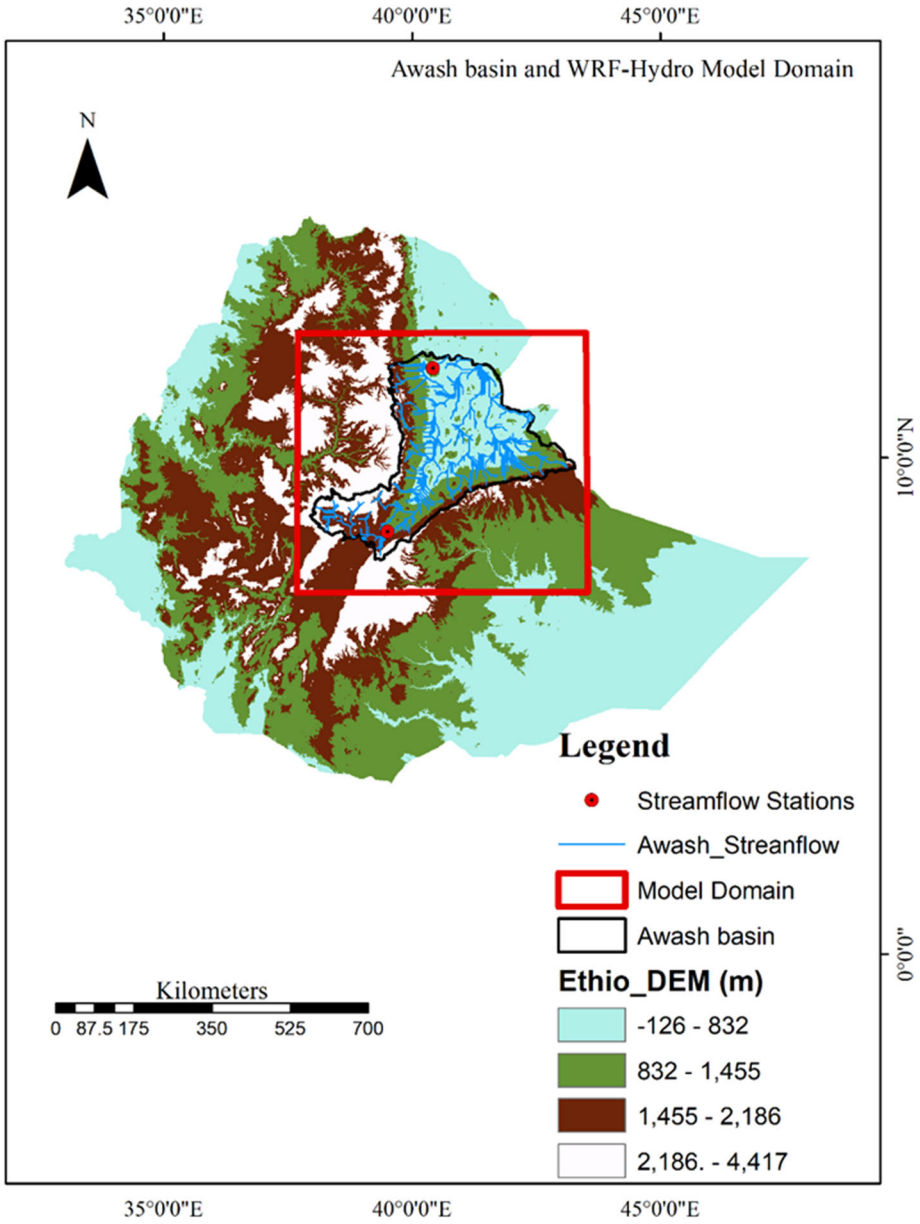


Figure 1. Awash Basin and WRF-Hydro Model Domain.

Temporal resolutions typically range from hourly to daily, depending on the study's objectives and the availability of input data. Higher temporal resolutions, such as hourly data, are beneficial for capturing the dynamics of rainfall events and their immediate impacts on runoff and streamflow, critical for effective water resource management in the basin [53].

2.3.3. Land Use Data Processing, Integration, and Simulation Design

The study's innovative coupling of LUC dynamics with high-resolution hydrologic modeling advances the understanding of anthropogenic changes in the Awash Basin. Systematically comparing 2001–2020 scenarios quantifies trade-offs between land use shifts (e.g., urbanization, agriculture) and water–energy fluxes, a template for similar basins. Integrating open-source tools (GEE, ArcGIS 10.4, Python 3.12, and WRF-Hydro v5.2) enhances reproducibility while focusing on process-based attribution (via scenario isolation), setting it apart from conventional sensitivity analyses. This approach bridges gaps in regional hydroclimatic studies and supports sustainable land-water management under changing LUC pressures.

Further model-specific preprocessing was required for compatibility with the WRF-Hydro/Noah-MP framework. The ESA CCI maps were first reclassified using ArcGIS 10.4 to align with the MODIS IGBP classification scheme adopted in WRF [54]. Then, using SAGA-GIS, the reclassified rasters were converted into a binary format compatible with the WRF Preprocessing System (WPS) to generate geo_em_d01_LUC.nc files via geogrid.exe. This preprocessing workflow ensured that each LUC scenario was spatially explicit, temporally consistent, and technically compatible with the coupled WRF-Hydro/Noah-MP system.

These feed into WPS to generate domain files ('geo_em_d01_LUC.nc') for each scenario, while GLDAS-forced meteorological data is gridded (via R) for consistency. WRF's 'real.exe' then produces scenario-specific initial conditions ('wrfinput_d01_LUC.nc'), combined with GIS-processed routing inputs, which drive the coupled WRF-Hydro/Noah-MP model (Figure 2). Crucially, the framework leverages multi-scenario simulations to isolate LUC effects, with calibration/validation against observed hydrometeorological data ensuring robustness.

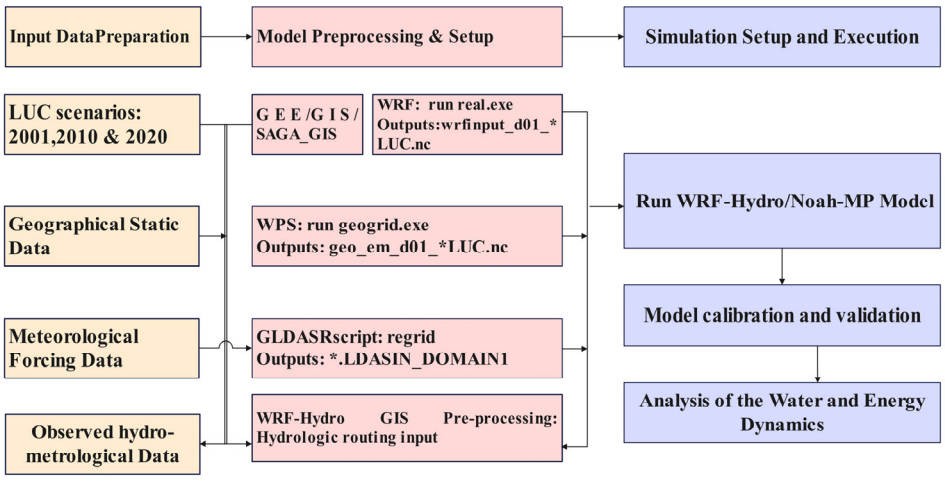


Figure 2. Methodological framework.

To assess the impact of land use change (LUC) on hydrological processes in the Awash Basin, this study integrates three distinct land use scenarios for 2001, 2010, and 2020. These scenarios depict the evolution of land cover over two decades, with each year capturing a snapshot of land use at that time. The 2001 scenario serves as the baseline, representing the initial land use conditions and helping establish a reference for comparison. The 2010 scenario reflects mid-term land use changes, marking the intermediate phase of anthropogenic and natural shifts in land cover [55]. Finally, the 2020 scenario captures the most recent land use dynamics, highlighting the effects of urbanization, agricultural expansion, and other human-induced transformations [56]. Using remote-sensing-derived

land use data, this study enables advanced analysis of LUCC scenarios, incorporating high-resolution satellite imagery and spatial data to quantify land cover changes over time [57]. This remote sensing integration significantly enhances the precision of land use change detection and its impacts on hydrological and energy fluxes, providing a robust methodology for assessing the influence of evolving land use on water resources across the Awash Basin [58,59].

To isolate the hydrological effects of decadal land use change from interannual climate variability, we conducted three distinct simulation experiments. Each experiment used the same meteorological forcing (GLDAS-2.1, 2000–2024) and model parameterization but was driven by a static land use map representing a specific snapshot in time: the 2001, 2010, and 2020 LULC scenarios, respectively. By comparing the outputs (e.g., ET, runoff) from these parallel simulations, we can directly attribute differences to the evolving land cover, as the climatic driver is held constant across them.

2.4. Land Use and Land Cover Change Analysis

To quantify and analyze the transitions between different land cover classes between 2010 and 2020, we employed Markov transition matrices. A Markov matrix is a square matrix that describes the probability of a land cover class transitioning to another class over a specified time period [60]. Each element P_{ij} of the matrix represents the proportion of area that changed from class *i* (in 2010) to class *j* (in 2020) [61]. This analysis was crucial for identifying dominant land conversion processes, such as cropland encroachment into woodlands or grassland fragmentation due to urbanization [62].

Furthermore, to analyze the spatial relationship between precipitation and elevation, we utilized multiple spatial interpolation techniques on observed station data (1990–2021). We compared four common methods:

- Inverse Distance Weighting (IDW): Assumes that points closer to the prediction location have more influence [63].
- Kriging: A geostatistical method that uses spatial correlation to provide a best linear unbiased estimate [64].
- Spline: Fits a mathematical surface that passes through the data points with minimal curvature.
- Thiessen Polygons: Assigns the value of the nearest station to all locations within its polygon, creating a discrete surface.

This comparative analysis allowed us to select the most appropriate representation of precipitation patterns for hydrological analysis in the topographically complex basin [65].

2.5. Model Performance Evaluation and Ground-Based Observations for Validation

The WRF-Hydro/NoahMP model for the Awash Basin was manually calibrated using key parameters that significantly influence hydrological processes. Given the basin's complexity, adjustments were made to parameters such as Manning's roughness coefficient (Manning), saturated hydraulic conductivity (Satdk), and the scaling factors for surface and subsurface runoff (DXRT, DTRT_CH, and DTRT_TER). These modifications were necessary to advance the model's capability to simulate streamflow dynamics accurately. The calibration process focused on optimizing the model outputs to match observed streamflow data, addressing discrepancies caused by variations in land cover, soil properties, and hydrometeorological conditions across the basin [66].

Model calibration and validation are critical to assess the accuracy of the WRF-Hydro model in simulating streamflow and overall water balance components. Observed streamflow data from in situ monitoring stations were used to calibrate and validate the model. Model performance was evaluated using statistical metrics such as the Nash-Sutcliffe Effi-

ciency (NSE), Root Mean Square Error (RMSE), and Bias [67,68]. These metrics help assess how well the model replicates observed streamflow and identify discrepancies in simulated water balance components. This validation process ensures that the WRF-Hydro model provides reliable simulations for water yield and extreme event prediction. Streamflow data, measured at gauging stations, are critical for validating model simulations of river discharge and assessing the overall water balance within basins [65,69,70].

$$R^2 = 1 - \frac{\sum_{i=1}^{n}(yi_{observed} - yi_{calculated})^2}{\sum_{i=1}^{n}(yi_{observed} - y_{obs\ mean})^2} \quad (1)$$

where $yi_{observed}$ is the observed value, $yi_{calculated}$ is the calculated value, and $y_{obs\ mean}$ is the mean of the observed values. An R^2 value closer to 1 indicates a better fit of the model to the observed data.

RMSE, on the other hand, quantifies the average magnitude of the errors between predicted and observed values, providing insight into the model's predictive accuracy. It is calculated as follows:

$$RMSE = \sqrt{\frac{1}{n}\sum_{i=1}^{n}(yi - yi, Obs\ mean)^2} \quad (2)$$

where n is the number of observations. Lower *RMSE* values show better model performance. *RMSE* and R^2 comprehensively assess model performance [71,72].

3. Results

3.1. WRF-Hydro/NoahMP Model Calibration and Validation Results

The WRF-Hydro/NoahMP model can simulate streamflow dynamics within the Awash Basin. Time series plots at Metehara (Figure 3) and Adaitu (Figure 4) stations indicate that the model effectively captures seasonal variability and the timing of major runoff events, closely aligning with observed hydrographs [64]. Notably, the scatter plots reveal strong correlations between observed and simulated streamflow, with R^2 values of 0.80 at Metehara (Figure 5) and 0.89 at Adaitu (Figure 6), underscoring the model's ability to explain a substantial portion of the variance in daily streamflow. These results affirm the model's proficiency in representing the basin's key hydrological processes, including rainfall-runoff transformation and flow routing.

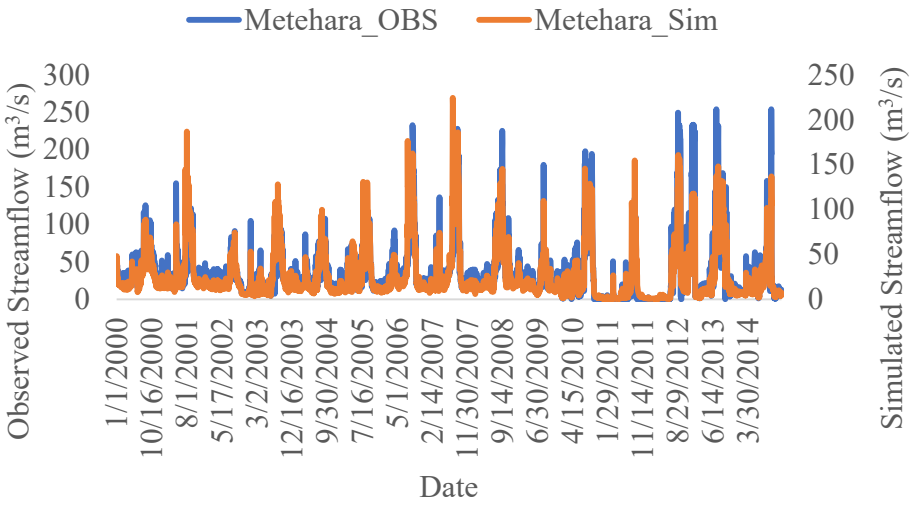


Figure 3. Metehara streamflow gauge station (2000–2014).

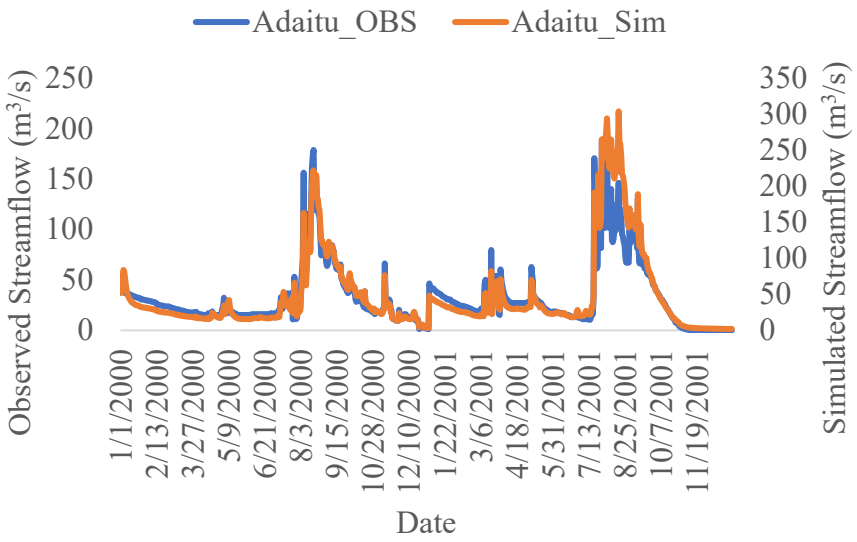


Figure 4. Adaitu streamflow gauge station (2000–2001).

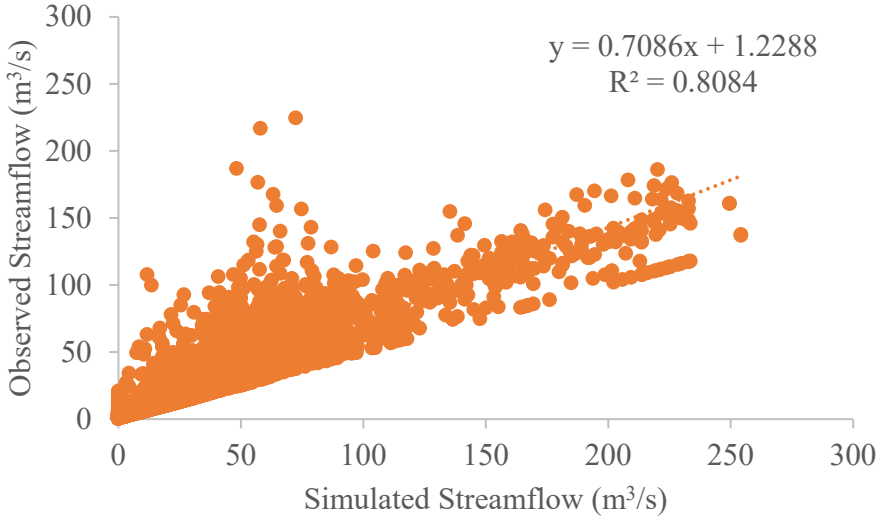


Figure 5. Linear regression of observed and simulated Metehara streamflow (2000–2014).

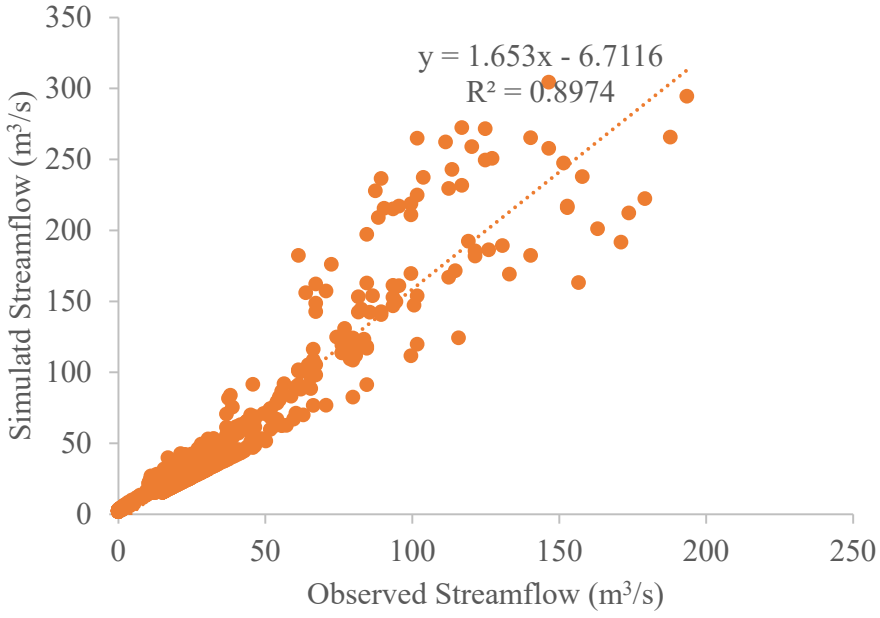


Figure 6. Linear regression of observed and simulated Adaitu streamflow (2000–2001).

These findings confirm that the WRF-Hydro/NoahMP framework is valuable and practical for simulating streamflow in the semi-arid Awash Basin. Nevertheless, further refinements, mainly targeted at extreme-event simulation, would enhance its utility for flood forecasting and water resource management in this data-scarce region [73].

3.2. Land Use and Land Cover Change Dynamics in Awash Basin (2000–2020)

Analysis of the multi-temporal ESA CCI land cover series revealed significant shifts that reflect natural and anthropogenic pressures (Figure 7). Over the past two decades, land cover changes in the Awash Basin have significantly impacted hydrological processes. The decadal land cover maps of the Awash Basin reveal a landscape in subtle yet significant flux, characterized by competing and spatially distinct processes of agricultural stability, vegetation change, and wetland decline. While major classes like Cropland (around 21%), Grassland (around 26%), and Shrubland (around 17%) exhibit remarkable stability in their overall basin-wide percentages across the two decades, this apparent stasis masks more dynamic underlying transitions. The most notable net changes include a persistent, accelerating increase in Woodland (from 3.2% to 4.6%) and a progressive expansion of Urban areas, coupled with the near-total disappearance of Wetlands (from 0.9% to 0.0%). This juxtaposition of afforestation/reforestation trends, likely occurring in the highlands, with the loss of critical wetland ecosystems and creeping urbanization in localized hotspots, paints a novel picture of a basin undergoing multifaceted environmental pressures that are not captured by analyzing any single land cover class in isolation.

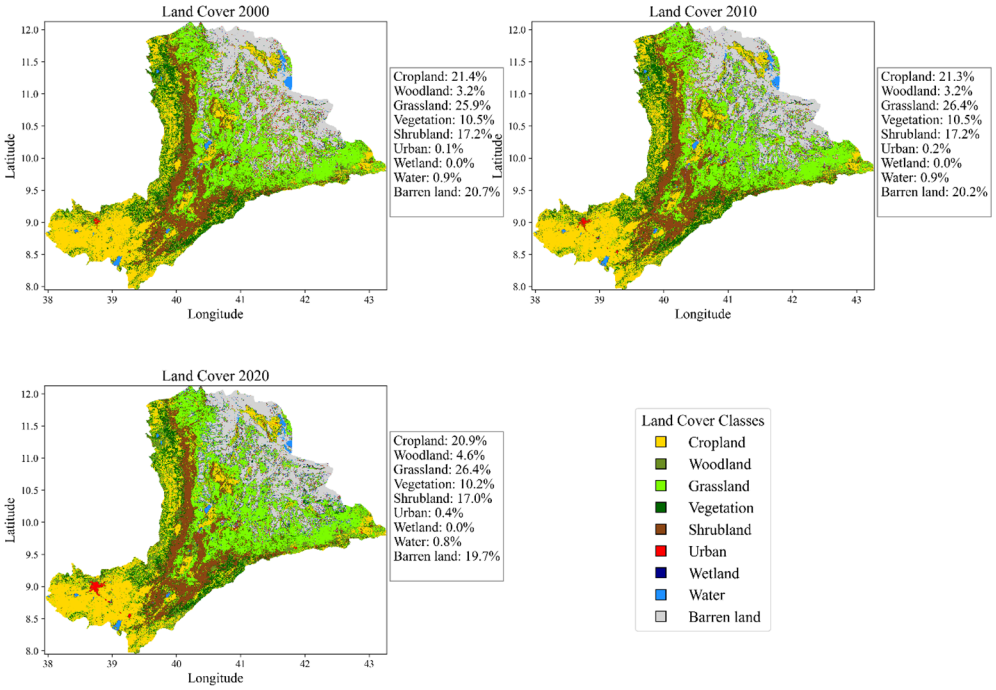


Figure 7. Land use and land cover area.

The substantial increase in woodland areas (Figure 8) from 2010 to 2020 might help mitigate some of these impacts by enhancing transpiration and stabilizing soil, but careful management is needed to balance economic development with environmental sustainability [74,75]. Understanding these dynamics is vital to the region's current water resource planning and sustainable land use practices.

As detailed in Section 2.4, Markov transition matrix analysis was applied to the ESA CCI land cover data to quantify transitions between 2010 and 2020 (Figure 9). The 2010–2020 transition matrix (Figure 9) reveals rapid cropland encroachment into woodlands

(13.9%) and grasslands (7.3%), mirroring Ethiopia's national agricultural GDP growth (6% annually [76]. However, this expansion coincides with degradation signals: shrublands, a transitional state for 26.7% of lost woodlands, show low persistence (58.5%), suggesting eventual conversion to barren land (12.0% of grassland transitions). Such shifts reduce infiltration capacity, exacerbating Awash's seasonal water scarcity [77,78]. Urbanization, though small in scale (1.0% persistence), fragments critical moisture-replenishing grasslands (26.4% of urban transitions), amplifying runoff in Addis Ababa's periphery [79]. These changes threaten irrigation-dependent agroeconomies downstream, where 60% of Ethiopia's sugar plantations rely on flows from the Awash River.

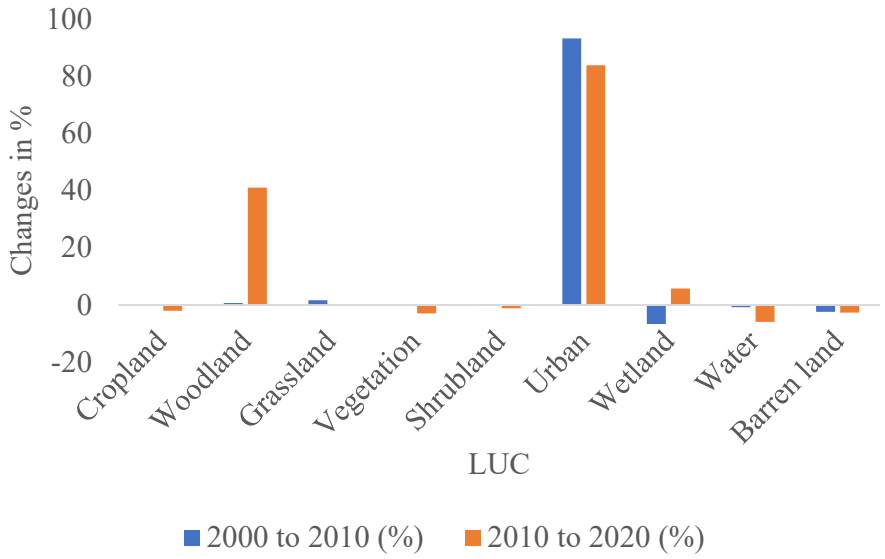


Figure 8. Land use and land cover change.

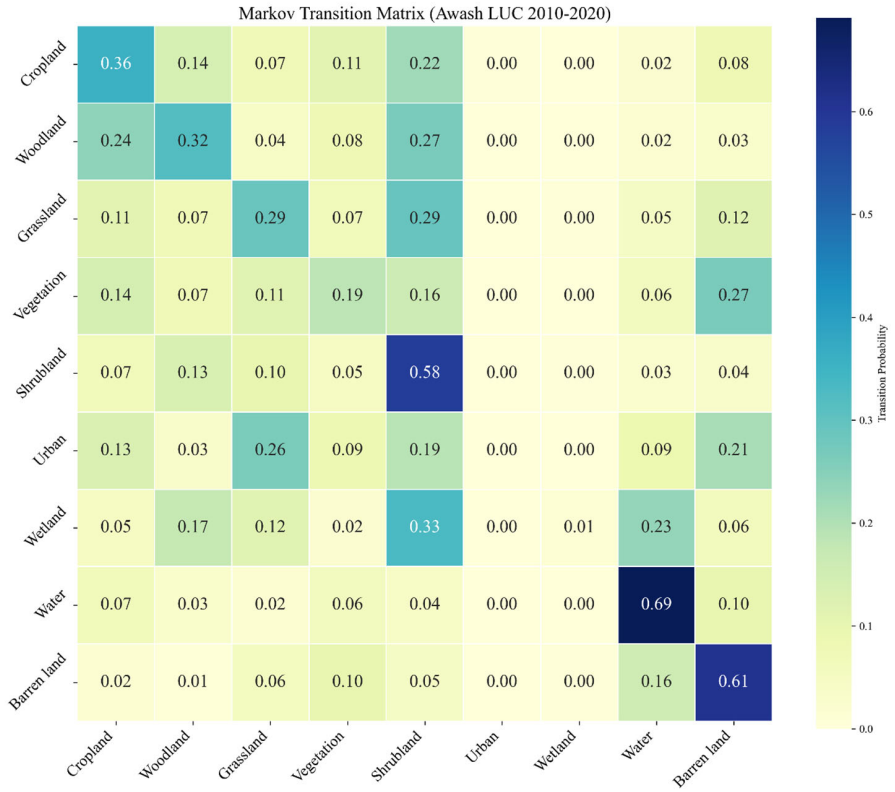


Figure 9. Markov transition matrices for the land cover from 2010 to 2020.

3.3. Crop Water Use Response to Land Use Change: Model Performance and Trend Analysis

The scatterplot reveals a nuanced performance of the WRF-Hydro/NoahMP model in simulating evapotranspiration (ET) dynamics for Ethiopia's Awash Basin. While the model demonstrates exceptional skill in capturing temporal patterns (R^2 = 0.75–0.88 across land use scenarios), matching GLEAM's observed seasonal variability and response to meteorological drivers, it systematically underestimates absolute ET magnitudes (Figure 10). This divergence suggests that the model's parameterizations, particularly for soil–vegetation–atmosphere interactions, may require calibration to better represent the basin's unique ecohydrological characteristics [80]. The robust pattern reproduction confirms the framework's utility for studying the relative impacts of land use change. However, the persistent low bias (points below the 1:1 line) indicates opportunities to refine vegetation resistance parameters, soil moisture thresholds, or precipitation partitioning to improve absolute flux estimates [53]. This dual behavior's strong correlation, combined with consistent underestimation, highlights both the model's capability for comparative scenario analysis and the need for region-specific adjustments to enhance its quantitative accuracy for water resource applications [81].

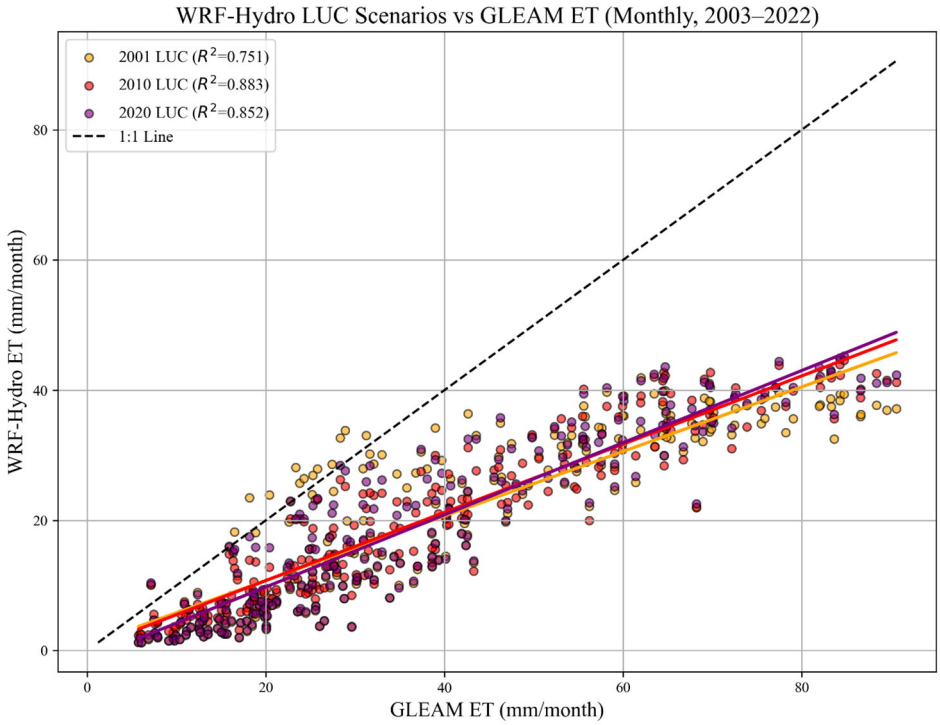


Figure 10. WRF-Hydro LUC Scenarios vs. GLEAM ET (2003–2022).

The model outputs demonstrated strong concordance with the GLDAS reference dataset, yielding monthly R^2 values of 0.96, 0.94, and 0.88 for the 2010, 2020, and 2001 LUC scenarios (Figure 11A). Annual R^2 values were similarly robust at 0.90, 0.83, and 0.80 (Figure 11B). These high correlation coefficients affirm the model's capability to accurately capture temporal ET dynamics, particularly under the 2010 LUC configuration. Such performance underscores the model's reliability for simulating land surface fluxes in data-scarce regions like the Awash Basin, aligning with previous studies validating WRF-Hydro's efficacy in semi-arid environments [82].

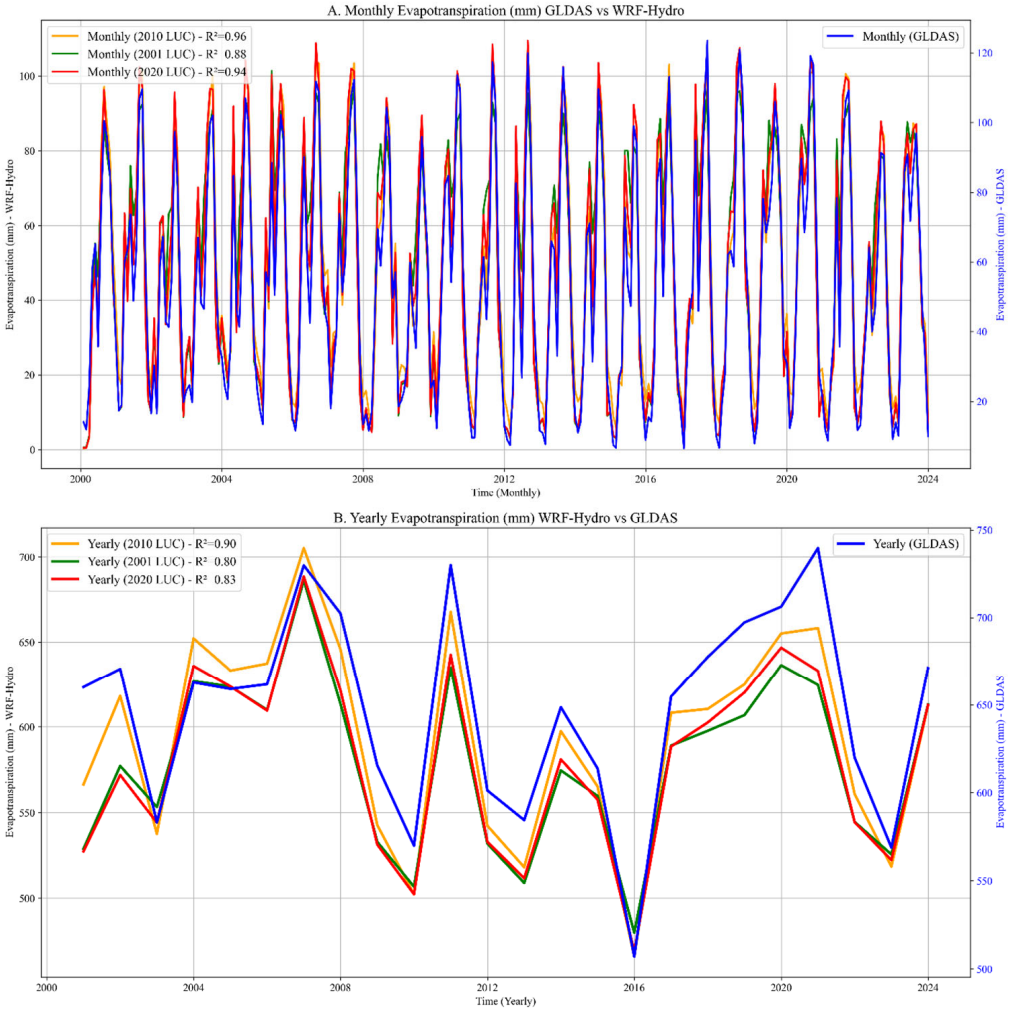


Figure 11. Monthly average and yearly comparison of ET trends under LUC scenarios with GLDAS.

The observed ET trends reflect the complex interplay between urbanization and land use changes over two decades. From 2001 to 2010, ET exhibited a moderate yearly decline (−0.323), driven by early urban expansion (+117.72 km^2) and cropland loss (−58.23 km^2), partially offset by modest woodland growth (+23.13 km^2). The monthly ET trend (0.005) suggests slight seasonal stability, likely due to remaining vegetation buffering and rapid ET loss. However, 2010–2020 saw the steepest yearly ET decline (−0.637), aligning with accelerated urbanization (+204.66 km^2) and severe cropland/shrubland losses (−458.46 km^2 and −209.88 km^2). Despite substantial woodland expansion (+1420.29 km^2), its ET contribution may have lagged, allowing urban effects to dominate. By 2020, the yearly ET decline softened (−0.111), indicating that mature woodlands began counteracting urban ET suppression, while the positive monthly trend (0.004) hints at recovering seasonal ET cycles due to increased forest cover [81,83]. These trends indicate a growing need for integrated land management strategies that consider ecological, hydrological, and socioeconomic dimensions, ultimately fostering a more resilient and sustainable land use framework for the Awash Basin. By supporting the Green Legacy Initiative and incorporating sustainable practices into urban and agricultural planning, Ethiopia can mitigate the impacts of urbanization and land use changes, promoting a more balanced coexistence between development and environmental conservation [84].

Urbanization was the primary driver of ET reduction, particularly in 2010–2020, when impervious surfaces expanded rapidly. However, the 2020 stabilization of ET decline suggests that large-scale woodland growth eventually mitigated urban impacts. Cropland and shrubland losses exacerbated ET declines, especially in the middle decade, while grassland changes had minimal influence. The monthly trends reveal that seasonal ET patterns remained resilient or improved (positive slopes in 2001 and 2020), likely due to the woodland's stronger transpiration in growing seasons. These findings underscore that while urbanization suppresses ET, strategic afforestation can partially restore regional water cycling, as seen in the 2020 data. Future land use policies should balance urban growth with woodland conservation to maintain sustainable ET regimes [85].

Evapotranspiration (ET) trends vary significantly with land use changes and climatic conditions. The Sen's Slope results for monthly and yearly ET provide insights into these trends. For the 2001 land use condition, the monthly Sen's Slope is slightly positive (0.005), indicating a slight increase in monthly ET, while the yearly slope is negative (−0.323), suggesting an overall decrease in yearly ET. This mixed trend could be due to the balance between vegetated areas and other land covers. In contrast, the 2010 land use condition shows a negative monthly slope (−0.003) and a more significantly negative yearly slope (−0.637), indicating a pronounced decrease in ET, possibly due to increased urbanization and decreased vegetated areas. In the 2020 LUC scenario, the monthly slope becomes slightly positive again (0.004), but the yearly slope remains negative (−0.111), suggesting a slight recovery in monthly ET trends but an ongoing decrease over the year [16,86].

The spatial change maps of evapotranspiration (ET) between the 2001–2010 and 2010–2020 periods reveal a nuanced hydrological response to land use/cover (LUC) dynamics in the Awash Basin. The widespread increase in ET from 2001 to 2010 (Figure 12B), especially in the western and central basins, aligns with documented agricultural expansion and conversion of natural vegetation to cropland and built-up areas [74]. Such transitions typically enhance evaporative demand and atmospheric water loss, as croplands and exposed soils often exhibit higher ET than forests or shrublands. This is supported by recent findings in the Modjo watershed (a major Awash tributary), where LULC change from forest/shrub to cropland and bare land led to increased ET and decreased surface runoff [74].

In contrast, the 2010–2020 period shows a marked decline in ET across much of the basin, particularly central and eastern regions (Figure 12A). This spatial pattern coincides with the continued expansion of built-up and barren land and a reduced vegetation cover, as reported for the upper and central Awash sub-basins. These land cover changes are associated with decreased soil moisture and reduced vegetative transpiration, resulting in lower ET. Simultaneously, such changes can increase infiltration and subsurface flow due to reduced surface sealing, as observed in the same studies. This shift in hydrological partitioning lowers ET, reduces surface runoff, and increases subsurface flow, underscoring the nonlinear and time-dependent nature of LUC impacts on water balance components in the Awash Basin [87].

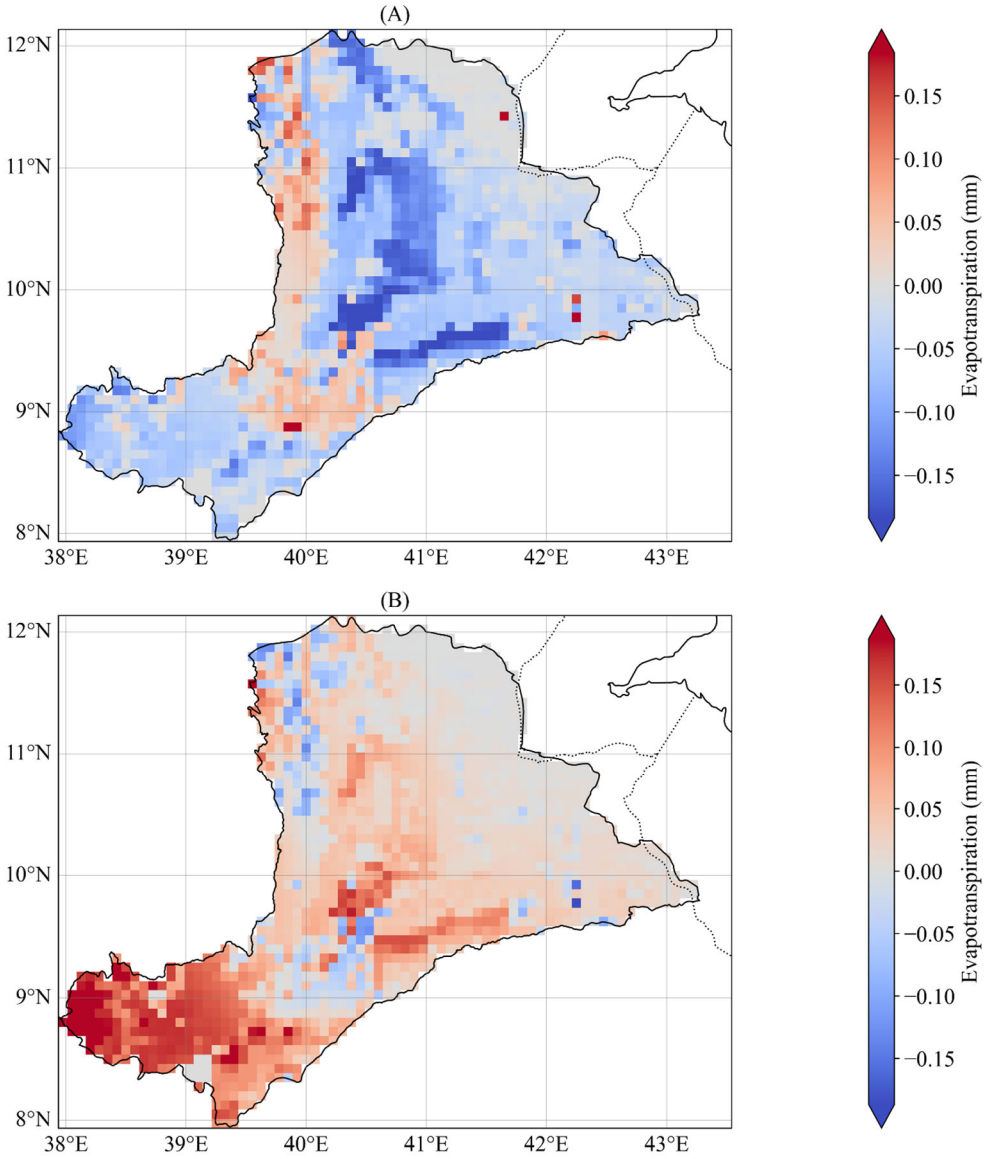


Figure 12. Spatial change maps of evapotranspiration under (**A**) 2020–2010 and (**B**) 2010–2001 LUC scenarios.

3.4. Implications of Land Use Change for Irrigation Water Sources

The simulated hydrological response to decadal Land Use Cover (LUC) changes reveals a significant shift in the primary sources of irrigation water in the Awash Basin. The transition from the 2001 to 2010 LUC scenario (Figure 13B), a period marked by agricultural expansion, predominantly stimulated increases in surface runoff, particularly in the western headwaters [8,88]. This suggests that the land cover shift during this decade promoted conditions that enhanced overland flow, potentially increasing water delivery to reservoirs and rivers used for large-scale surface irrigation schemes.

This trend reversed during the subsequent 2010–2020 LUC transition (Figure 13A), a period characterized by substantial woodland recovery. The maps show a significant decrease in surface runoff across the basin's central and western portions, coinciding with a pronounced and widespread increase in subsurface flow (Figure 13C). This shift indicates that the 2020 LUC scenario enhanced infiltration and groundwater recharge, a crucial process for sustaining soil moisture and well-based irrigation. The model simulates opposing trajectories in runoff partitioning across consecutive decades due solely to LUC changes [3]. This highlights a critical trade-off for water managers: agricultural expansion

may boost immediate surface water availability, while afforestation promotes long-term groundwater sustainability, albeit potentially reducing direct surface flow.

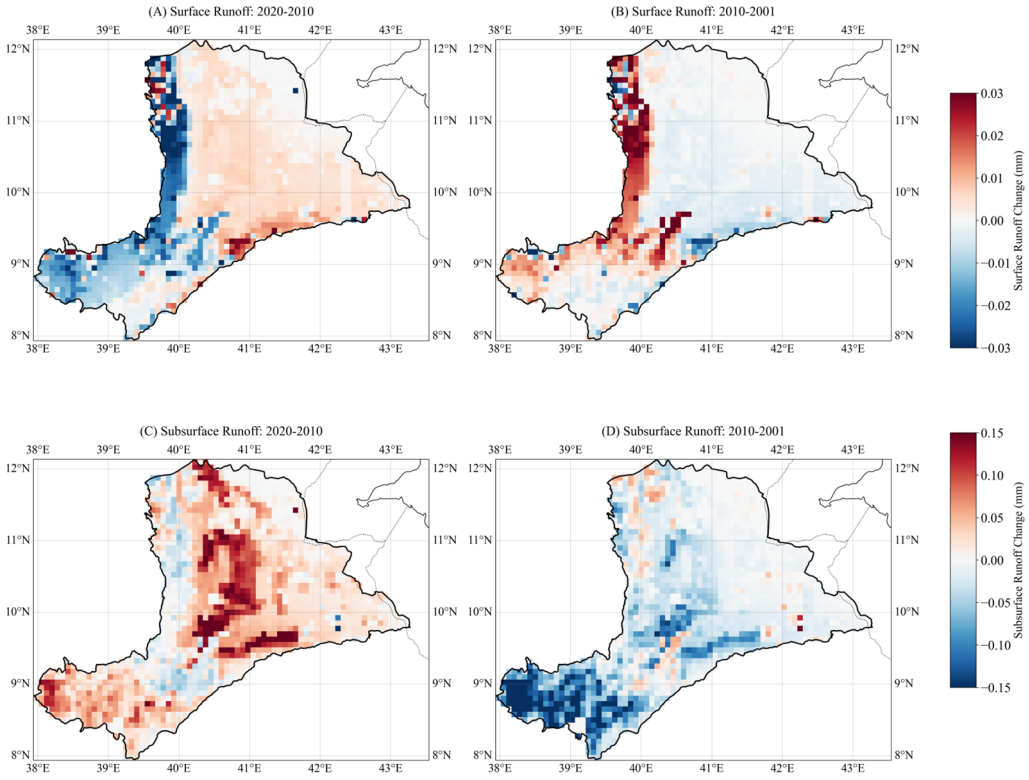


Figure 13. Spatial change maps of surface and subsurface runoff.

This trend reverses during the subsequent 2010–2020 LUC transition (Figure 13A). The maps show a significant decrease in surface runoff across the basin's large central and western portions, coinciding with a pronounced, widespread increase in subsurface runoff (Figure 13D), primarily along the central basin axis. This simulated shift points towards the 2020 LUC scenario, representing land surface characteristics that enhance infiltration and promote water movement through subsurface routes (potentially indicating vegetation recovery, changes in agricultural practices, or different soil parameterization linkages), consequently reducing direct overland flow. The novel aspect here is the model's simulation of opposing trajectories in runoff partitioning across consecutive decades due solely to LUC changes; the system does not simply trend towards more or less total runoff but fundamentally reorganizes how runoff is generated, highlighting the critical need to analyze both surface and subsurface components to understand the full hydrological consequence of land cover dynamics [5].

3.5. WRF-Hydro/NoahMP Precipitation Simulation Evaluation

The comparison of WRF-Hydro simulations using the 2001 land use configuration with ERA5 precipitation data reveals a notable difference in temporal-resolution performance. The higher monthly (Figure 14A) R^2 value of 0.80 suggests that the model captures seasonal precipitation patterns with greater fidelity, likely driven by its ability to represent the timing and magnitude of individual rainfall events. In contrast, the lower yearly R^2 (Figure 14B) of 0.66 indicates challenges in accurately simulating interannual precipitation variability, highlighting potential limitations in capturing longer-term climatic drivers or multi-year land-atmosphere feedbacks that influence precipitation totals within the Awash Basin.

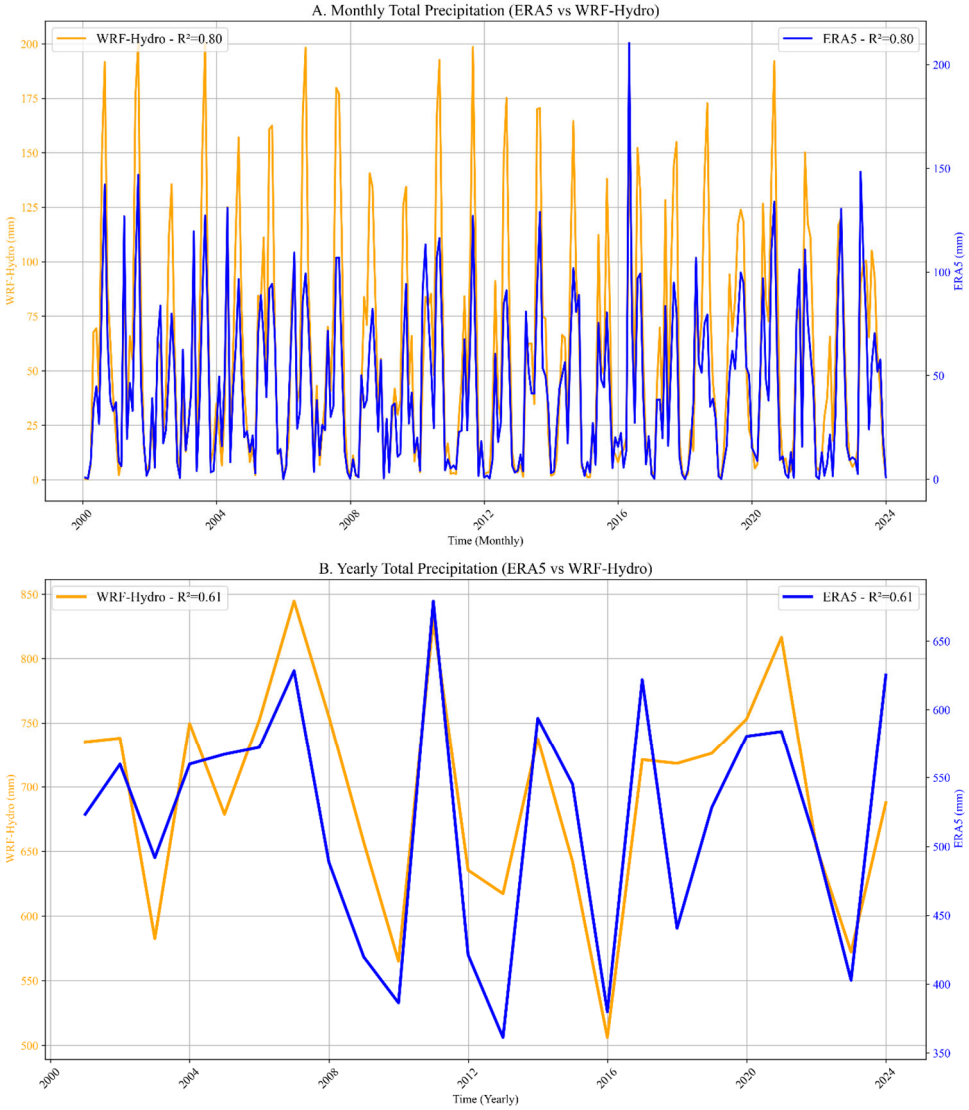


Figure 14. Precipitation comparison.

The Awash Basin in Ethiopia exhibits a distinct relationship between elevation and precipitation, as demonstrated by a linear regression of precipitation data from 1990 to 2021 across 13 stations (Figure 15). The scatter plot shows a positive correlation: higher elevations receive greater average annual precipitation. This trend aligns with the basin's diverse climatic zones, ranging from semi-arid lowlands to humid highlands. For instance, areas above 2500 m typically receive rainfall exceeding 1400 mm annually, while regions below 500 m experience less than 200 mm (Figure 16). The regression model achieved an R^2 value of 0.850, indicating a strong linear relationship between elevation and precipitation. Such findings are crucial for understanding the basin's hydrological dynamics, which rely heavily on rainfall for agriculture and water resource management [89,90].

The observed precipitation data in the Awash Basin reveal significant spatial and temporal variability. Locations in the upper basin, such as Abomsa and AA Bole, exhibit higher precipitation levels, often exceeding 1000 mm annually, while the middle and lower basins, represented by Metehara and Adaitu, receive substantially less rainfall, typically below 600 mm and 400 mm, respectively. This gradient reflects the basin's diverse climate, influenced by topography and regional weather patterns. The data also shows interannual variability, with some years experiencing notably higher or lower precipitation than others, highlighting the importance of understanding these fluctuations for effective water resource management.

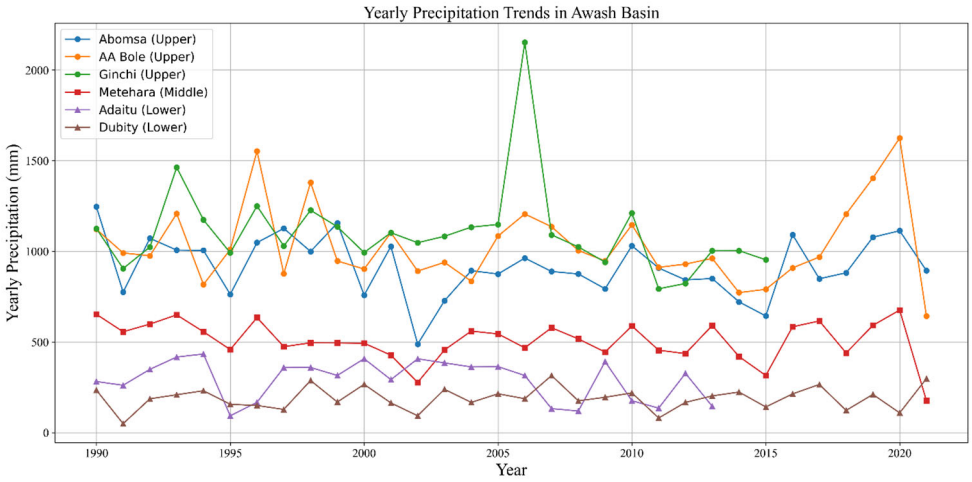


Figure 15. Yearly precipitation trends in the Awash Basin.

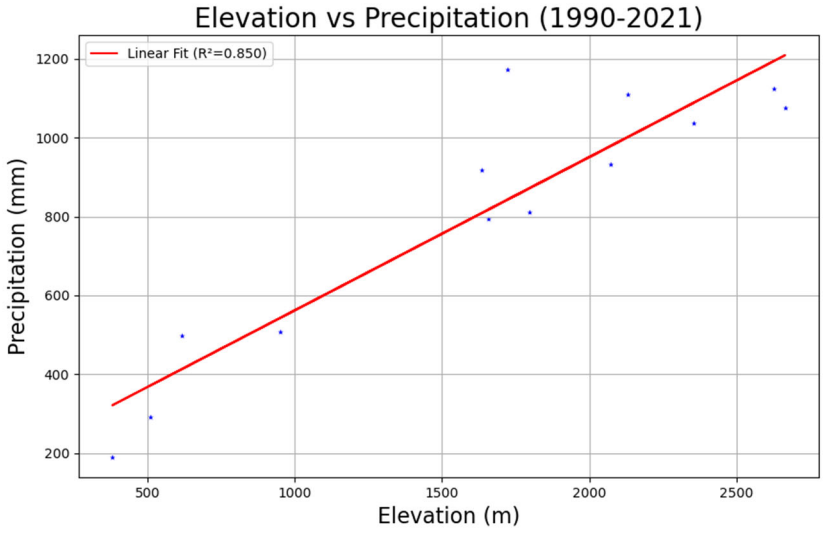


Figure 16. Precipitation and elevation correlation in the Awash Basin.

This scatter plot reveals a strong positive relationship between elevation and precipitation across the Awash Basin from 1990 to 2021, as indicated by the linear fit with an R^2 value of 0.85. The apparent upward trend suggests that higher-elevation areas consistently receive greater rainfall, likely due to orographic effects that enhance moisture condensation as air masses rise over elevated terrain. This robust correlation underscores the dominant role of topography in shaping the basin-wide precipitation distribution, highlighting the importance of incorporating elevation-driven rainfall gradients into hydrological models and water resource planning for regions with complex terrain like the Awash.

These comparative spatial maps illustrate the diversity of precipitation patterns across the Awash Basin, which are estimated using four interpolation techniques: IDW, Kriging, Spline, and Thiessen (Figure 17). Each method reveals distinct spatial gradients and localized precipitation features, underscoring how the choice of interpolation method can influence hydrological assessments. Kriging and IDW produce smooth, continuous surfaces that highlight subtle spatial variability and local maxima, while spline interpolation generates broader, more generalized gradients. In contrast, the Thiessen method produces distinct, abrupt zones of influence around each station, thereby emphasizing its discrete nature. The differences among these methods underscore the importance of selecting an appropriate interpolation technique, as it can significantly affect the representation of

precipitation fields and, consequently, water resource analysis and decision-making in data-scarce basins such as the Awash.

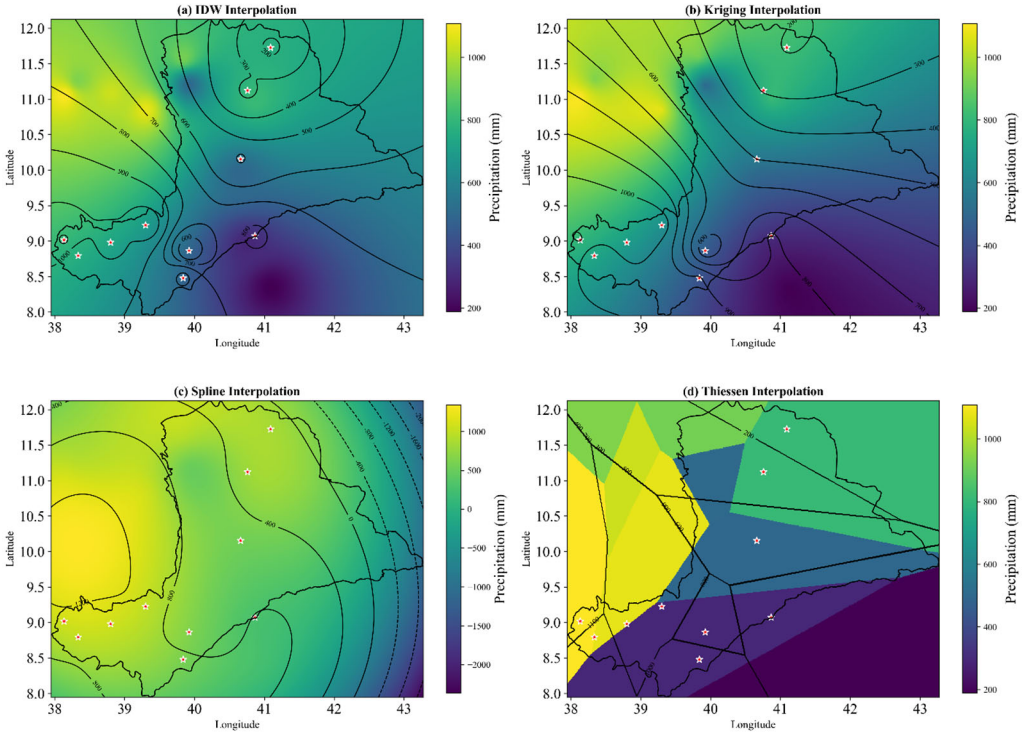


Figure 17. Comparative interpolation techniques. Note: Stars are stations location.

3.6. Model Performance in Simulating Latent Heat Flux: Seasonal Fidelity Versus Interannual Divergence

As depicted in Figure 18A, the latent heat flux (LE) analysis in the Awash Basin reveals a pronounced dominance of seasonality in both the WRF-Hydro/NoahMP simulations (across three LUC scenarios) and the GLDAS reference product. The monthly linear regression of the model and GLDAS (R^2: 0.75–0.83) indicates that both modeling frameworks adeptly capture the seasonal cycle of LE, which is primarily governed by the region's bimodal rainfall regime driven by the migration of the Intertropical Convergence Zone (ITCZ) and associated variations in solar radiation [88]. This seasonal predictability is a hallmark of the Awash Basin, where precipitation and energy fluxes are tightly coupled to the timing of Belg and Kiremt rains and orographic and altitudinal gradients [91]. The close alignment at monthly scales suggests that WRF-Hydro and GLDAS are well-constrained by meteorological forcing and land surface seasonality in simulating the timing and magnitude of evapotranspiration and related energy exchanges.

However, the much lower yearly R^2 values (0.25–0.47) highlight a substantial divergence in the models' capacity to reproduce interannual variability in latent heat flux (Figure 18B). This discrepancy points to structural or parametric differences in how WRF-Hydro/NoahMP and GLDAS represent slower processes such as soil moisture memory, vegetation physiological responses, and the handling of extreme hydroclimatic events, all of which modulate year-to-year water and energy partitioning in the basin [92]. Notably, the GLDAS product exhibits larger interannual swings than any WRF-Hydro scenario, suggesting that GLDAS may be more sensitive to precipitation anomalies or employ different land surface parameterizations and data assimilation schemes. While land use change (LUC) scenarios within WRF-Hydro influence annual LE (with the 2010 scenario showing the highest correlation with GLDAS), the inter-model differences are more pronounced than the intra-model LUC effects. This underscores the importance of considering model

structural uncertainty alongside land use and climate inputs when evaluating water and energy budgets in data-scarce, highly variable basins like the Awash [74].

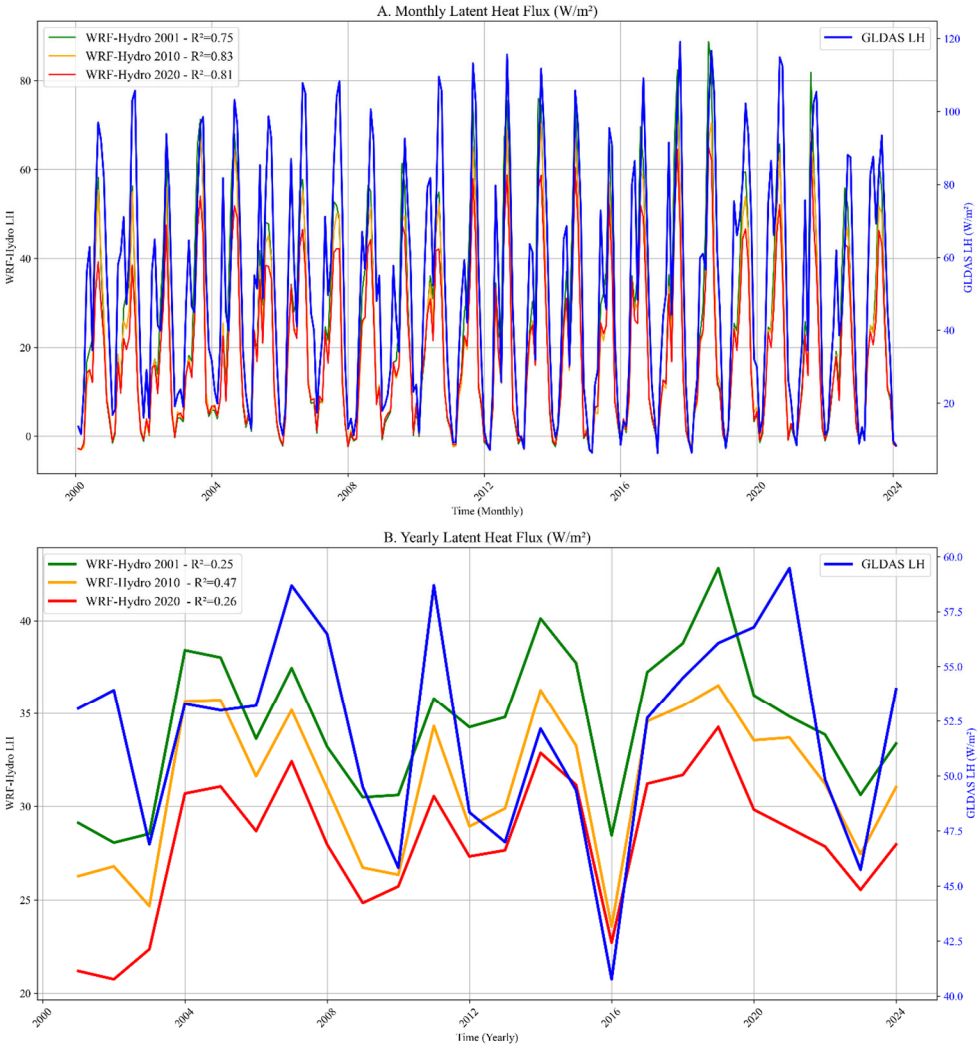


Figure 18. Latent heat flux (W/m^2): (**A**) monthly average and (**B**) yearly sum.

3.7. Reversal in Latent Heat Flux Trends Driven by Successive Land Use Changes

The spatial evolution of simulated latent heat flux (LH), which represents the energy consumed by evapotranspiration, reveals a complex, nonlinear response of the WRF-Hydro/NoahMP model to decadal land use and land cover (LUC) changes across the Awash Basin. The comparison of LH fields across the three LUC scenarios, 2001, 2010, and 2020, highlights not only the model's sensitivity to surface representation but also reveals spatially divergent trends in evaporative dynamics.

Transitioning from the 2001 to 2010 LUC scenario results in a basin-wide decline in LH (Figure 19B), particularly across the central and western zones, where extensive blue-dominant regions signal a reduction in evaporative energy [93]. This suggests that, within the 2010 LUC framework, the modeled land surface exhibited lower transpiration efficiency, potentially due to reduced vegetation density, shifts toward land cover types with lower leaf area indices, or increased land degradation. These reductions in LH may also reflect altered soil properties or a decline in agricultural intensity, limiting the land surface's ability to partition net radiation into latent heat [94].

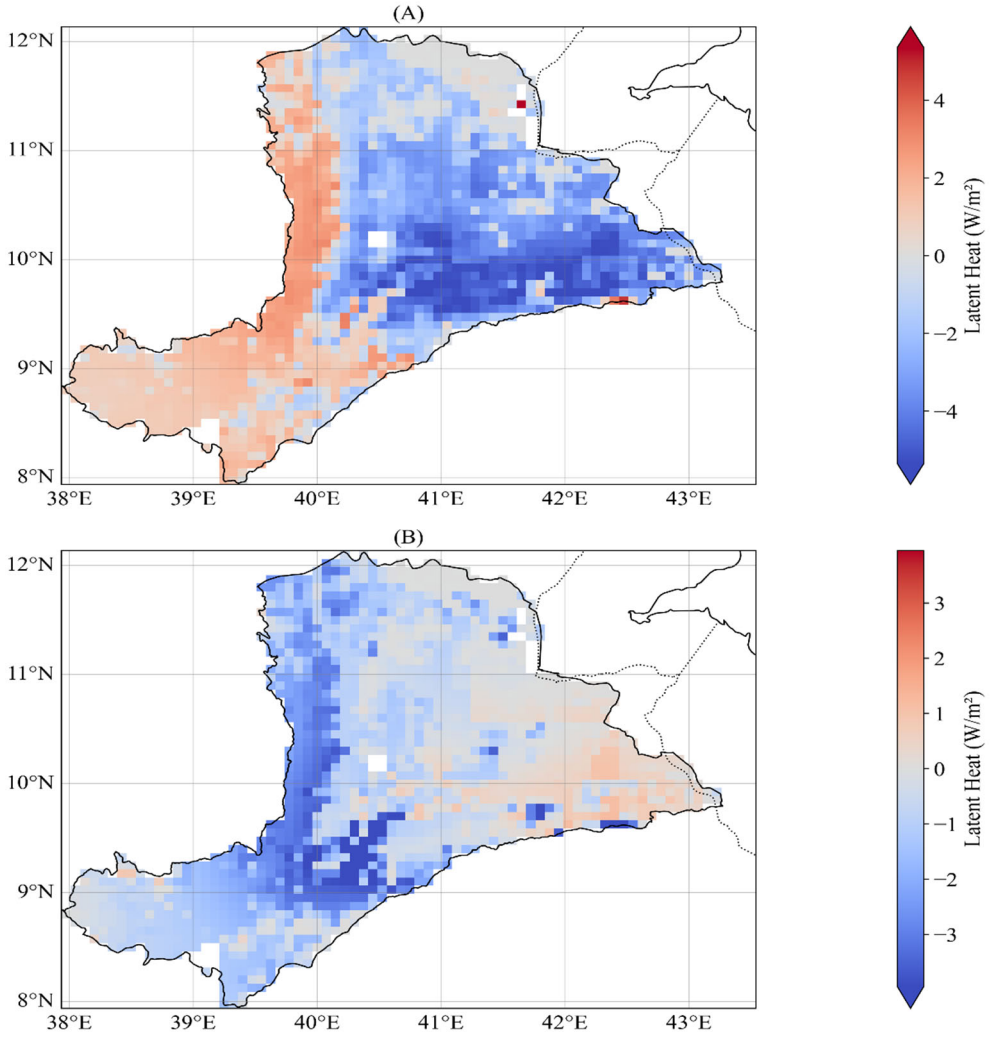


Figure 19. Spatial evaluation of simulated latent heat flux (LH) in (**A**) 2020–2010 and (**B**) 2010–2001 LUC scenarios.

In stark contrast, the transition from the 2010 to 2020 scenario shows a robust, spatially coherent increase in LH across much of the basin, especially in the western highlands and southern sectors (Figure 19A). The predominance of red-shaded areas in the spatial change maps indicates that the 2020 LUC state allowed enhanced evaporative processes. This may be attributed to vegetation recovery, afforestation efforts, land management changes, or increased irrigation coverage, amplifying the latent heat component of the surface energy balance by facilitating moisture availability and transpiration [95].

This observed temporal oscillation in LH—first a suppression, then a resurgence—underscores the model's high sensitivity to LUC dynamics and illustrates the nonlinear nature of land-atmosphere interactions. Notably, the spatial footprints of change are not uniformly distributed, suggesting that different sub-regions of the basin are undergoing distinct ecological and anthropogenic transitions. These findings carry important implications: they highlight the potential for land use policy and management strategies to modulate local and regional hydroclimatic feedback by shifting evapotranspiration [32].

This analysis reveals that decadal land use transitions in the Awash Basin impart measurable, non-uniform impacts on latent heat fluxes. The modeled response depends on the areal extent of land use change and the functional characteristics of altered land surfaces, underscoring the importance of accurately capturing LUC types and their biophysical properties in future modeling efforts.

4. Discussion

This study integrates multi-decadal land use change (LUC) scenarios into the WRF-Hydro/Noah-MP framework to assess their impact on water resources critical to agriculture in the Awash Basin. The results offer significant insights into how land use changes—particularly agricultural expansion, urbanization, and afforestation—have shaped the availability of surface and subsurface water for irrigation over the past two decades. The findings enhance our understanding of land-water interactions in a key agricultural region and provide a dynamic, scenario-driven approach to inform sustainable water management in agriculture.

4.1. Principal Findings in the Context of Study Objectives

This study hypothesized that multi-decadal land use and land cover (LULC) changes are a primary driver of alterations in the partitioning of water resources between surface and subsurface stores, with direct consequences for agricultural water management in the Awash Basin. By integrating observed LULC scenarios (2001, 2010, 2020) into the WRF-Hydro/Noah-MP model, we isolated the hydrological effects of land transformation from climate variability. Our findings robustly support this hypothesis and provide clear answers to our specific objectives:

(Objective 1) Impact of LULC on Hydrologic Processes: We found a fundamental shift in runoff generation mechanisms. The early period (2001–2010), characterized by the rapid expansion of cropland and urbanization, led to increased surface runoff. This was reversed in the later period (2010–2020), dominated by woodland recovery, which promoted subsurface flow at the expense of surface runoff [8].

(Objective 2) Trade-offs in Water Fluxes: A critical trade-off was identified. Agricultural expansion favors immediate surface water availability for large-scale irrigation, while afforestation enhances long-term groundwater sustainability for small-scale and well-based irrigation, albeit potentially reducing reservoir inflows [25].

(Objective 3) Implications for Management: The results provide a quantitative evidence base for spatially targeted land use planning [96], demonstrating how initiatives like Ethiopia's Green Legacy Initiative can be optimized to secure irrigation water without compromising other water-dependent sectors [31].

4.2. Impact of Land Use Change on Hydrological and Energy Processes

The integration of land use scenarios from 2001, 2010, and 2020 into the WRF-Hydro/Noah-MP model reveals the significant role of LUC in altering hydrological and energy processes across the Awash Basin [80]. Our findings suggest that agricultural expansion between 2001 and 2010 increased surface runoff, while urbanization further exacerbated runoff dynamics from 2010 to 2020. These trends align with previous studies, which have shown that agricultural intensification and urban expansion tend to increase runoff and alter the partitioning of water resources, particularly in semi-arid regions [3,83].

Urbanization and agricultural expansion in Ethiopia have led to significant wetland loss, with unregulated demand driving a decline in wetland persistence from 99.4% in 2000–2010 to 1.1% in 2010–2020. Wetlands transitioning to open water due to sedimentation from upland deforestation reduce their peak-flow buffering capacity, exacerbating flood risks [97]. Concurrently, urban sprawl, such as Addis Ababa's expansion into grasslands, intensifies heat islands and increases heat fluxes, potentially reducing rainfall—a critical moisture source for Ethiopia's rainfed agriculture [98]. This urban warming and wetland loss compound economic risks by stressing the water–energy–food nexus, potentially costing Ethiopia a significant portion of its GDP each year if current land use trends continue [2,74].

In contrast, the afforestation efforts observed between 2010 and 2020 resulted in a substantial increase in woodland cover, which contributed to a decrease in surface runoff and an increase in subsurface flow. This suggests that reforestation, as part of Ethiopia's Green Legacy Initiative, plays a critical role in mitigating the impacts of urbanization and agricultural expansion by enhancing soil moisture retention and promoting groundwater recharge [31]. These findings support the notion that afforestation and sustainable land management practices can provide viable solutions to mitigate the adverse effects of rapid urbanization and agricultural expansion on hydrological processes [30].

4.3. Evapotranspiration and Energy Flux Dynamics: Model Performance and Biophysical Drivers

The results also demonstrate how land use change affects evapotranspiration (ET) and latent heat flux (LE) in the basin. Our study showed a strong seasonal alignment between simulated ET and observations from GLEAM and GLDAS, with high R^2 values indicating the model's ability to capture temporal variability. However, the model systematically underestimated ET, which may be due to limitations in its representation of soil-vegetation-atmosphere interactions, as discussed in previous studies [82,84]. This persistent underestimation could be attributed to uncertainties in the model's parameterizations for semi-arid vegetation, such as stomatal conductance or soil moisture stress functions, or may reflect biases in the meteorological forcing data over regions with sparse ground observations. The discrepancy in ET magnitude suggests that while the model captures the relative changes in ET under different LUC scenarios, further calibration is needed to improve its quantitative accuracy [16,86]. Future research should focus on refining the model's parameterizations for soil moisture, leaf area index (LAI), and vegetation resistance to better represent the unique ecohydrological characteristics of the Awash Basin.

The impact of LUC on water fluxes was particularly notable in the transition from 2001 to 2010, where the decline in ET and surface runoff coincided with increased urbanization and agricultural intensification [92]. This supports the finding that urbanization suppresses ET and alters runoff pathways. In contrast, the transition from 2010 to 2020, marked by woodland recovery, resulted in a spatially coherent increase in subsurface flow and a stabilization of ET, indicating that regrowth of vegetation can enhance groundwater recharge and sustain ecosystem water use [74]. These results underscore the importance of vegetation cover in regulating the water cycle, highlighting a complex trade-off in the Awash Basin, where both cropland and forests compete for the same water resources.

4.4. Implications for Water Resource Management

The findings of this study have significant implications for agricultural water management in the Awash Basin and similar semi-arid regions [73,99]. The results emphasize the need for integrated land use and water management strategies that account for the hydrological trade-offs among different land covers. Our study highlights the potential of afforestation to enhance groundwater recharge, which can benefit well-based irrigation but may concurrently reduce surface runoff feeding large reservoirs. Conversely, unchecked cropland expansion increases surface water yield but at the risk of soil degradation and reduced infiltration. Therefore, strategic land use planning is essential in the context of Ethiopia's Green Legacy Initiative, which aims to increase forest cover [30,31]. By incorporating these hydrological trade-offs into water management strategies, policymakers can implement practical measures such as targeted afforestation to enhance groundwater recharge, improved irrigation techniques to reduce water wastage, and land use zoning to protect critical water sources, all of which promote more sustainable agricultural practices that balance food production with the conservation of water resources.

4.5. Limitations of the Scientific Approach and Future Research Directions

While our integrated modeling framework represents a significant advance, several limitations must be acknowledged, pointing the way for future research:

1. Static Land Use Representation: Using static snapshots of LULC for multi-year simulations overlooks intra-annual dynamics, such as crop rotation and seasonal leaf area index changes. Future work should incorporate dynamic vegetation models to enhance the accuracy of predictions.
2. Exclusion of Human Water Management: The model does not simulate water abstractions for irrigation or reservoir operations. Coupling WRF-Hydro with a water resources management model would provide a more realistic representation of the managed water balance. The absence of irrigation abstractions and reservoir regulation means our simulations represent a 'naturalized' hydrological response to LULC change. In reality, the significant water withdrawals for agriculture in the Awash Basin likely alter the partitioning of surface and subsurface flows we have identified. Therefore, coupling WRF-Hydro with a water resources management model is a critical next step to quantify the combined effects of LULC change and direct human water use on the competition for agricultural water sources.
3. Uncertainty in Validation Data: The GLDAS and GLEAM products used for validation contain their own uncertainties, which may contribute to the observed model biases. A more robust validation using denser ground-based observations, when available, would be beneficial.
4. Future Scenarios: This study analyzed historical changes. A critical next step is to combine projected future LULC scenarios (e.g., continued urbanization, planned afforestation) with climate change projections to assess the long-term sustainability of agricultural water resources in the Awash Basin.

5. Conclusions

This study quantified the profound impact of multi-decadal land use and land cover (LULC) change on the availability and partitioning of agricultural water sources in the Awash Basin, Ethiopia. By integrating satellite-derived LULC scenarios (2001, 2010, 2020) into the WRF-Hydro/Noah-MP modeling framework, we isolated the hydrological effects of land transformation from climate variability. The principal conclusions are as follows:

1. LULC changes directly control the primary source of irrigation water. The main changes were rapid cropland expansion and urbanization (2001–2010), followed by significant woodland recovery (2010–2020). These trajectories caused a fundamental shift in the basin's hydrological regime:
    - The 2001–2010 period, characterized by agricultural and urban expansion, consistently saw an increase in surface runoff. This trend enhances potential water storage in reservoirs, favoring large-scale, surface-water irrigation schemes.
    - The 2010–2020 period, characterized by substantial woodland recovery, promoted infiltration and subsurface flow, thereby enhancing groundwater recharge. This shift benefits small-scale and well-based irrigation by strengthening baseflow and soil moisture reserves.
2. Evapotranspiration (ET) and energy fluxes are highly sensitive to LULC. Urbanization was the primary driver of suppressed ET and latent heat, while subsequent woodland recovery facilitated their resurgence. This confirms that vegetation cover is a critical regulator of the basin's water and energy balance, with afforestation contributing to a more moderated local climate through enhanced evaporative cooling.

3. The WRF-Hydro/Noah-MP framework is a powerful tool for strategic water planning in data-scarce regions. The model demonstrated strong performance in simulating streamflow (R^2 = 0.80–0.89) and capturing seasonal patterns of water and energy fluxes, providing a reliable platform for scenario analysis despite a noted tendency to underestimate absolute ET magnitudes.

Practical Implications for Agricultural Water Conservation:

The primary utility of this research lies in its ability to inform strategic land and water management, thereby conserving water for agricultural use. The demonstrated trade-off means that land use planning is a direct form of water resource management. To apply these findings:

- ✓ For Surface Water Conservation: Managing land use in upstream catchments that feed major reservoirs. Limiting extensive impervious surfaces and promoting sustainable agricultural practices in these specific sub-basins can help maintain reliable surface runoff for large-scale irrigation.
- ✓ For Groundwater Conservation: Strategically target afforestation and woodland conservation in recharge zones and areas where small-scale irrigation is prevalent. This will enhance infiltration, directly replenishing the aquifers and soil moisture that these farmers depend on.
- ✓ For Integrated Planning: Use this modeling framework as a decision-support tool to pre-test the hydrological consequences of future land use plans, such as the Green Legacy Initiative, ensuring that afforestation goals are achieved without unintended negative impacts on downstream surface water irrigation.

In conclusion, securing water for agriculture in the Awash Basin requires a nuanced understanding of how specific land use changes alter the water cycle. This study provides the evidence base to move from reactive water management to proactive land use planning, where decisions about crops, forests, and cities are made with their direct impact on irrigation water sources in mind.

Author Contributions: T.M.G.: Methodology, Data curation, Software, Formal analysis, Investigation, Visualization, Writing—original draft, Writing—review and editing. B.C.: Conceptualization, Supervision, Project administration, Resources, Methodology, Validation, Writing—review and editing, Funding acquisition. H.Z.: Data curation, Software, Writing—review and editing. J.S.: Methodology, Data curation, Resources, Writing—review and editing. All authors have read and agreed to the published version of the manuscript.

Funding: This research is funded by the Science and Technology Project of Jiangsu Provincial Department of Natural Resources (No. JSZRKJ202421), the National Natural Science Foundation of China (No. 4245000217), Strategic Priority Research Program of the Chinese Academy of Sciences (Category B, Geographic Intelligence, No. XDB0740300), the Jiangsu Province's Special Fund for Carbon Peak and Carbon Neutrality Technological Innovation for the year 2023 (No. BE2023855) and the Lianyungang Key R&D Program (Industrial Foresight and Key Core Technologies, No. 22CY080).

Data Availability Statement: The original contributions presented in this study are included in the article. Further inquiries can be directed to the corresponding authors.

Acknowledgments: During the preparation of this work, the authors used Grammarly for grammar and style checking. After using this tool, the authors reviewed and edited the content as needed and take full responsibility for the content of the publication.

Conflicts of Interest: The authors declare no conflicts of interest.

References

1. Ghiat, I.; Mackey, H.R.; Al-Ansari, T. A Review of Evapotranspiration Measurement Models, Techniques and Methods for Open and Closed Agricultural Field Applications. *Water* **2021**, *13*, 2523. [CrossRef]
2. Negese, A. Impacts of Land Use and Land Cover Change on Soil Erosion and Hydrological Responses in Ethiopia. *Appl. Environ. Soil Sci.* **2021**, *2021*, 15–17. [CrossRef]
3. Getahun, Y.S.; HAJ, V.L. Assessing the Impacts of Land Use-Cover Change on Hydrology of Melka Kuntrie Subbasin in Ethiopia, Using a Conceptual Hydrological Model. *J. Waste Water Treat. Anal.* **2015**, *6*, 1000210. [CrossRef]
4. Gebrechorkos, S.H.; Bernhofer, C.; Hülsmann, S. Climate Change Impact Assessment on the Hydrology of a Large River Basin in Ethiopia Using a Local-Scale Climate Modelling Approach. *Sci. Total Environ.* **2020**, *742*, 140504. [CrossRef]
5. Tadese, M.T.; Kumar, L.; Koech, R.; Zemadim, B. Hydro-Climatic Variability: A Characterisation and Trend Study of the Awash River Basin, Ethiopia. *Hydrology* **2019**, *6*, 35. [CrossRef]
6. Heyi, E.A.; Dinka, M.O.; Mamo, G. Assessing the Impact of Climate Change on Water Resources of Upper Awash River Sub-Basin, Ethiopia. *J. Water L. Dev.* **2022**, *52*, 232–244. [CrossRef]
7. ARBA Awash Basin Authority. Executive Summary of Strategic River Basin Plan for Awash Basin. 2017, pp. 1–53. Available online: https://www.cmpethiopia.org/content/download/2841/11761/file/Main%20report%20final%20June%202017..pdf (accessed on 1 July 2025).
8. Bihonegn, B.G.; Awoke, A.G. Evaluating the Impact of Land Use and Land Cover Changes on Sediment Yield Dynamics in the Upper Awash Basin, Ethiopia the Case of Koka Reservoir. *Heliyon* **2023**, *9*, e23049. [CrossRef]
9. Assega, M.A.; Nigussie, A.B.; Womber, Z.R.; Amognehegn, A.E.; Yeniakal, A.E.; Hassen, H.A. Evaluation of Hydrological Models for Streamflow Prediction: A Case Study of the Mille River, Lower Awash Basin, Ethiopia. *Int. J. River Basin Manag.* **2024**, 1–13. [CrossRef]
10. Tekleab, S.G.; Kassew, A.M. Hydrologic Responses to Land Use/Land Cover Change in the Kesem Watershed, Awash Basin, Ethiopia. *J. Spat. Hydrol.* **2019**, *15*, 2.
11. Mercer, A.; Dyer, J. Identification of Dominant Warm-Season Latent Heat Flux Patterns in the Lower Mississippi River Alluvial Valley. *Procedia Comput. Sci.* **2021**, *185*, 1–8. [CrossRef]
12. Verri, G.; Pinardi, N.; Gochis, D.; Tribbia, J.; Navarra, A.; Coppini, G.; Vukicevic, T. A Meteo-Hydrological Modelling System for the Reconstruction of River Runoff: The Case of the Ofanto River Catchment. *Nat. Hazards Earth Syst. Sci.* **2017**, *17*, 1741–1761. [CrossRef]
13. Chen, C.J.; Chi, M.H.; Ye, J.R. Assessing Hydroclimate Response to Land Use/Cover Change Using Coupled Atmospheric-Hydrological Models. *Geosci. Lett.* **2023**, *10*, 54. [CrossRef]
14. Ma, S.; Wang, L.J.; Jiang, J.; Zhao, Y.G. Land Use/Land Cover Change and Soil Property Variation Increased Flood Risk in the Black Soil Region, China, in the Last 40 Years. *Environ. Impact Assess. Rev.* **2024**, *104*, 107314. [CrossRef]
15. Wang, D.; Liu, Y.; Yu, T.; Zhang, Y.; Liu, Q.; Chen, X.; Zhan, Y. A Method of Using WRF-Simulated Surface Temperature to Estimate Daily Evapotranspiration. *J. Appl. Meteorol. Climatol.* **2020**, *59*, 901–914. [CrossRef]
16. Xing, W.; Feng, Z.; Cao, X.; Fu, J.; Wang, W. Urbanization Impacts on Evapotranspiration Change across Seven Typical Urban Agglomerations in China. *Sci. Total Environ.* **2024**, *950*, 175399. [CrossRef]
17. Ajami, H. Geohydrology: Global Hydrological Cycle. In *Encyclopedia of Geology*, 2nd ed.; Academic Press: Oxford, UK, 2021; pp. 393–398. ISBN 978-0-08-102909-1.
18. Huang, J.; Zhu, X.Y.; Lu, J.; Sun, Y.; Zhao, X.Q. Effects of Different Land Use Types on Microbial Community Diversity in the Shizishan Mining Area. *Huanjing Kexue/Environ. Sci.* **2019**, *40*, 5550–5560. [CrossRef]
19. Schmied, H.M.; Eisner, S.; Franz, D.; Wattenbach, M.; Portmann, F.T.; Flörke, M.; Döll, P. Sensitivity of Simulated Global-Scale Freshwater Fluxes and Storages to Input Data, Hydrological Model Structure, Human Water Use and Calibration. *Hydrol. Earth Syst. Sci.* **2014**, *18*, 3511–3538. [CrossRef]
20. Rui, H.L.; Beaudoing, H. README Document for NASA GLDAS Version 2 Data Products. *Goddard Earth Sci. Data Inf. Serv. Cent. (GES DISC)* **2020**, *16*, 1–32.
21. Gochis, D.J.; Barlage, M.; Cabell, R.; Casali, M.; Dugger, A.; Fitzgerald, K.; Mcallister, M.; Mccreight, J.; Rafieeinasab, A.; Read, L.; et al. The NCAR WRF-Hydro® Modeling System Technical Description Until Further Notice, Please Cite the WRF-Hydro® Modeling System as Follows. 2020. Available online: https://wrf-hydro.readthedocs.io/en/latest/ (accessed on 1 July 2025).
22. NCAR. How To Build & Run WRF-Hydro V5 in Standalone Mode And Create Customized Geographical Inputs & Regrid Forcing Data. 2018, pp. 1–34. Available online: https://www.google.com/url?sa=t&source=web&rct=j&opi=89978449&url=https://ral.ucar.edu/sites/default/files/public/HowToBuildandRunWRF-HydroV5inStandaloneMode_0.pdf (accessed on 1 June 2025).
23. Naabil, E.; Lamptey, B.L.; Arnault, J.; Kunstmann, H.; Olufayo, A. Water Resources Management Using the WRF-Hydro Modelling System: Case-Study of the Tono Dam in West Africa. *J. Hydrol. Reg. Stud.* **2017**, *12*, 196–209. [CrossRef]
24. Taye, M.T.; Haile, A.T.; Dessalegn, M. *Flood Adaptation and Mitigation in the Awash Basin: Responding to New Climate Patterns*; University of Oxford: Oxford, UK, 2024; pp. 1–44.

25. Malede, D.A.; Andualem, T.G.; Yibeltal, M.; Alamirew, T.; kassie, A.E.; Demeke, G.G.; Mekonnen, Y.G. Climate Change Impacts on Hydroclimatic Variables over Awash Basin, Ethiopia: A Systematic Review. *Discov. Appl. Sci.* **2024**, *6*, 27. [CrossRef]
26. Abdulahi, S.D.; Abate, B.; Harka, A.E.; Husen, S.B. Response of Climate Change Impact on Streamflow: The Case of the Upper Awash Sub-Basin, Ethiopia. *J. Water Clim. Chang.* **2022**, *13*, 607–628. [CrossRef]
27. Haile, A.T.; Gebremedhin, M.A.; Rientjes, T.; Habib, E.; Langan, S.; Fenta, A.A. Assessment of Climate Change Impact on Flood Frequency Distributions in Baro Basin, Ethiopia. *Atmos. Res.* **2017**, *161–162*, 1305–1321.
28. Getahun, Y.S.; Li, M.H.; Chen, Y.Y.; Yate, T.A. Drought Characterization and Severity Analysis Using GRACE-TWS and MODIS Datasets: A Case Study from the Awash River Basin (ARB), Ethiopia. *J. Water Clim. Chang.* **2023**, *14*, 516–542. [CrossRef]
29. Ayenew, T. Water Management Problems in the Ethiopian Rift: Challenges for Development. *J. Afr. Earth Sci.* **2007**, *48*, 222–236. [CrossRef]
30. Green Legacy of Ethiopia, WWF 9, March 2022. Available online: https://www.ideassonline.org/public/pdf/EthiopiaGreenLegacy-ENG.pdf (accessed on 1 July 2025).
31. Campaign, B.T.; Nations, U.; Program, E. The Green Legacy Campaign in Ethiopia Setting a New World Record of Tree Seedlings Planted. *Green Leg. Initiat. Off. Prime Minist. Website Artic.* **2019**.
32. Alemu, M.G.; Wubneh, M.A.; Sahlu, D.; Zimale, F.A. Spatiotemporal Change of Climate Extremes under the Projection of CMIP6 Model Analysis over Awash Basin, Ethiopia. *Sustain. Water Resour. Manag.* **2023**, *9*, 195. [CrossRef]
33. Report, A.S. *Report on Findings from the Awash River Basin Who We Are*; University of Oxford: Oxford, UK, 2020; pp. 1–32.
34. Mirshafee, S.; Ansari, H.; Davary, K.; Ziaei, A.N.; Faridhosseini, A.; Choi, Y.S. Estimation of Water Balance Components by Noah-MP Land Surface Model for the Neyshaboor Watershed, Khorasan Razavi, Iran. *Appl. Water Sci.* **2024**, *14*, 22. [CrossRef]
35. Zhang, Y.; Kong, D.; Gan, R.; Chiew, F.H.S.; McVicar, T.R.; Zhang, Q.; Yang, Y. Coupled Estimation of 500 m and 8-Day Resolution Global Evapotranspiration and Gross Primary Production in 2002–2017. *Remote Sens. Environ.* **2019**, *222*, 165–182. [CrossRef]
36. Assimila-, D.; County, B.; County, B.; Springs, C.; Springs, C.; Branch, S. The Global Land Data. *Bull. Am. Meteorol. Soc.* **2004**, *85*, 381–394. [CrossRef]
37. Zarekarizi, M. Ensemble Data Assimilation for Flood Forecasting in Operational Settings: From Noah-MP to WRF-Hydro and the National Water Model. *Diss. Theses* **2018**.
38. P Roduct User Guide. 2017, pp. 1–52. Available online: https://www.esa-landcover-cci.org/?q=node/199 (accessed on 1 February 2025).
39. Miralles, D.G.; Bonte, O.; Koppa, A.; Baez-Villanueva, O.M.; Tronquo, E.; Zhong, F.; Beck, H.E.; Hulsman, P.; Dorigo, W.A.; Verhoest, N.E.C.; et al. GLEAM4: Global land evaporation and soil moisture dataset at 0.1° resolution from 1980 to near present. *Sci. Data* **2025**, *12*, 416. [CrossRef]
40. Zheng, C.; Jia, L.; Hu, G. Global Land Surface Evapotranspiration Monitoring by ETMonitor Model Driven by Multi-Source Satellite Earth Observations. *J. Hydrol.* **2022**, *613*, 128444. [CrossRef]
41. Conway, D. The Climate and Hydrology of the Upper Blue Nile River. *Geogr. J.* **2000**, *166*, 49–62. [CrossRef]
42. Haile, G.G. Irrigation in Ethiopia, a Review. *Acad. J. Agric. Res.* **2015**, *5*, 141–148.
43. Gemechu, T.M.; Zhao, H.; Bao, S.; Yangzong, C.; Liu, Y.; Li, F.; Li, H. Estimation of Hydrological Components under Current and Future Climate Scenarios in Guder Catchment, Upper Abbay Basin, Ethiopia, Using the SWAT. *Sustainability* **2021**, *13*, 9689. [CrossRef]
44. Andualem, T.G.; Guadie, A.; Belay, G.; Ahmad, I.; Dar, M.A. Hydrological Modeling of Upper Ribb Watershed, Abbay Basin, Ethiopia. *Glob. NEST J.* **2020**, *22*, 158–164.
45. Berhanu, B.; Seleshi, Y.; Melesse, A.M. Surface Water and Groundwater Resources of Ethiopia: Potentials and Challenges of Water Resources Development. In *Nile River Basin*; Springer: Berlin/Heidelberg, Germany, 2014; pp. 97–117.
46. Givati, A.; Service, I.H. Using the WRF-Hydro Model for 100 Years Flood Event in Israel Motivations—Developing Flood Warning System at a Country (Regional) Scale—Predictions of Peak Discharges and Water Volumes vs. It Return Periods and Exceedance Probabilities. Available online: https://cesmma.unical.it/wrf-hydro2014/pdf/WRF%20Hydro-Israel.pdf (accessed on 1 June 2025).
47. e Silva, I.A.; Rodriguez, D.A.; Espíndola, R.P. Improving Physiological Simulations in Seasonally Dry Tropical Forests with Limited Measurements. *Theor. Appl. Climatol.* **2024**, *155*, 7133–7146. [CrossRef]
48. dos Santos, J.A.; Campoe, O.C.; de Souza, C.R.; Marrichi, A.H.C.; Carneiro, R.L.; da Silva, P.H.M.; de Mattos, E.M.; Otto, M.S.G.; Gonsalez, B.T. Stomatal Conductance Models in Brazilian Forest Plantations: Genotype and Environmental Effects on Eucalypt and Pine Forests. *New For.* **2023**, *55*, 417–440. [CrossRef]
49. Gochis, D.; Yates, D.; Dugger, A.; Sampson, K.; Rasmussen, R.; Zhang, Y.; Cabell, R.; Rafieeinasab, A. WRF-Hydro / NoahMP Applications in Real-Time, Operational Hydrologic Forecasting Outline: WRF-Hydro System Description New Evolutions. 2023. Available online: https://ral.ucar.edu/sites/default/files/docs/session1gochismay23.pdf (accessed on 1 July 2025).
50. Sakaguchi, K.; Zeng, X. Effects of Soil Wetness, Plant Litter, and under-Canopy Atmospheric Stability on Ground Evaporation in the Community Land Model (CLM3.5). *J. Geophys. Res. Atmos.* **2009**, *114*, 1–14. [CrossRef]

51. Niyogi, D.S.; Raman, S. Comparison of Four Different Stomatal Resistance Schemes Using FIFE Observations. *J. Appl. Meteorol.* **1997**, *36*, 903–917. [CrossRef]
52. Huang, Y.; Bárdossy, A.; Zhang, K. Sensitivity of Hydrological Models to Temporal and Spatial Resolutions of Rainfall Data. *Hydrol. Earth Syst. Sci.* **2019**, *23*, 2647–2663. [CrossRef]
53. Github, U.N.; He, C. Noah-MP Land Surface Model Tutorial • Noah-MP Brief History and Recent Activities. 2024. Available online: https://ral.ucar.edu/sites/default/files/docs/noahmp_tutorial_ams_cenlinhe_27jan2024.pdf (accessed on 1 July 2025).
54. Sulla-Menashe, D.; Friedl, M.A. *User Guide to Collection 6 MODIS Land Cover (MCD12Q1 and MCD12C1) Product*; USGS: Reston, VA, USA, 2018; pp. 1–18.
55. Huang, S.; Gan, Y.; Chen, N.; Wang, C.; Zhang, X.; Li, C.; Horton, D.E. Urbanization Enhances Channel and Surface Runoff: A Quantitative Analysis Using Both Physical and Empirical Models over the Yangtze River Basin. *J. Hydrol.* **2024**, *635*, 131194. [CrossRef]
56. Ibu, B.; Dibandingkan, H.; Suplementasi, D.; Besi, Z.A.T.; Asam, D.A.N. Policy Brief 1 Policy Brief 1. 2023, 1, pp. 1–6. Available online: https://www.researchgate.net/publication/368450412_Green_Legacy_Initiative_for_Sustainable_Development?enrichId=rgreq-df644d53cc36a1ef875fa2956b5b65ee-XXX&enrichSource=Y292ZXJQYWdlOzM2ODQ1MDQxMjtBUzoxMTQzMTI4MTExOTY0MzIyOUAxNjc2MTQ1MjkwMDM3&el=1_x_2&_esc=publicationCoverPdf (accessed on 1 August 2025).
57. Ahmad, S.; Waseem, M.; Wahab, H.; Khan, A.Q.; Jehan, Z.; Ahmad, I.; Leta, M.K. Assessing Water Demand and Supply in the Upper Indus Basin Using Integrated Hydrological Modeling under Varied Socioeconomic Scenarios. *Appl. Water Sci.* **2025**, *15*, 5. [CrossRef]
58. Gu, H.; Ke, Y.; Bai, Z.; Ma, D.; Wu, Q.; Sun, J.; Yang, W. Improving Hydrological Simulations with a Dynamic Vegetation Parameter Framework. *Water* **2024**, *16*, 3335. [CrossRef]
59. Koczot, K.M.; Markstrom, S.L.; Hay, L.E. Effects of Baseline Conditions on the Simulated Hydrologic Response to Projected Climate Change. *Earth Interact.* **2011**, *15*, 1–23. [CrossRef]
60. Chen, L.; Sun, Y.; Saeed, S. Monitoring and Predicting Land Use and Land Cover Changes Using Remote Sensing and GIS Techniques—A Case Study of a Hilly Area. *PLoS ONE* **2018**, *13*, e0200493.
61. Hu, Y.; Zhen, L.; Zhuang, D. Assessment of Land-Use and Land- Cover Change in Guangxi, China. *Sci. Rep.* **2019**, *9*, 2189. [CrossRef]
62. Gashaw, T.; Tulu, T.; Argaw, M.; Worqlul, A.W. Modeling the Hydrological Impacts of Land Use/Land Cover Changes in the Andassa Watershed, Blue Nile Basin, Ethiopia. *Sci. Total Environ.* **2018**, *619–620*, 1394–1408. [CrossRef]
63. Gebremichael, H.B.; Raba, G.A.; Beketie, K.T.; Feyisa, G.L.; Siyoum, T. Changes in Daily Rainfall and Temperature Extremes of Upper Awash Basin, Ethiopia. *Sci. Afr.* **2022**, *16*, e01173. [CrossRef]
64. Wang, W.; Liu, J.; Xu, B.; Li, C.; Liu, Y.; Yu, F. A WRF/WRF-Hydro Coupling System with an Improved Structure for Rainfall-Runoff Simulation with Mixed Runoff Generation Mechanism. *J. Hydrol.* **2022**, *612*, 128049. [CrossRef]
65. Dinku, T.; Ceccato, P.; Grover-Kopec, E.; Lemma, M.; Connor, S.J.; Ropelewski, C.F. Validation of Satellite Rainfall Products over East Africa's Complex Topography. *Int. J. Remote Sens.* **2007**, *28*, 1503–1526. [CrossRef]
66. Sofokleous, I.; Bruggeman, A.; Camera, C.; Eliades, M. Grid-Based Calibration of the WRF-Hydro with Noah-MP Model with Improved Groundwater and Transpiration Process Equations. *J. Hydrol.* **2023**, *617*, 128991. [CrossRef]
67. Yang, S.; Zeng, J.; Fan, W.; Cui, Y. Evaluating Root-Zone Soil Moisture Products from GLEAM, GLDAS, and ERA5 Based on In Situ Observations and Triple Collocation Method over the Tibetan Plateau. *J. Hydrometeorol.* **2022**, *23*, 1861–1878. [CrossRef]
68. Ritter, A.; Muñoz-Carpena, R. Performance Evaluation of Hydrological Models: Statistical Significance for Reducing Subjectivity in Goodness-of-Fit Assessments. *J. Hydrol.* **2013**, *480*, 33–45. [CrossRef]
69. Ahmed, J.S.; Buizza, R.; Dell'Acqua, M.; Demissie, T.; Pè, M.E. Evaluation of ERA5 and CHIRPS Rainfall Estimates against Observations across Ethiopia. *Meteorol. Atmos. Phys.* **2024**, *136*, 17. [CrossRef]
70. Diro, G.T.; Grimes, D.I.F.; Black, E.; O'Neill, A.; Pardo-Iguzquiza, E. Evaluation of Reanalysis Rainfall Estimates over Ethiopia. *Int. J. Climatol.* **2009**, *29*, 67–78. [CrossRef]
71. Chai, T.; Draxler, R.R. Root Mean Square Error (RMSE) or Mean Absolute Error (MAE)?—Arguments against Avoiding RMSE in the Literature. *Geosci. Model Dev.* **2014**, *7*, 1247–1250. [CrossRef]
72. Lewis-Beck, M.; Bryman, A.; Futing Liao, T. R-Squared. *SAGE Encycl. Soc. Sci. Res. Methods* **2012**, 1187–1190. [CrossRef]
73. Tedla, H.Z.; Taye, E.F.; Walker, D.W.; Haile, A.T. Evaluation of WRF Model Rainfall Forecast Using Citizen Science in a Data-Scarce Urban Catchment: Addis Ababa, Ethiopia. *J. Hydrol. Reg. Stud.* **2022**, *44*, 101273. [CrossRef]
74. Besha, K.Z.; Demissie, T.A.; Feyessa, F.F. Effects of Land Use/Land Cover Change on Hydrological Responses of a Watershed in the Central Rift Valley of Ethiopia. *Hydrol. Res.* **2024**, *55*, 83–111. [CrossRef]
75. Kayitesi, N.M.; Guzha, A.C.; Mariethoz, G. Impacts of Land Use Land Cover Change and Climate Change on River Hydro-Morphology—A Review of Research Studies in Tropical Regions. *J. Hydrol.* **2022**, *615*, 128702. [CrossRef]
76. Teklay, A.; Dile, Y.T.; Asfaw, D.H.; Bayabil, H.K.; Sisay, K. Impacts of Climate and Land Use Change on Hydrological Response in Gumara Watershed, Ethiopia. *Ecohydrol. Hydrobiol.* **2021**, *21*, 315–332. [CrossRef]

77. Daba, M.H.; You, S. Quantitatively Assessing the Future Land-Use/Land-Cover Changes and Their Driving Factors in the Upper Stream of the Awash River Based on the CA–Markov Model and Their Implications for Water Resources Management. *Sustainability* **2022**, *14*, 1538. [CrossRef]
78. Zhang, X.; Lark, T.J.; Clark, C.; Yuan, Y.; Stephen, D. Carbon Losses in the US Midwest between 2008 and 2016. *Environ. Res. Lett.* **2022**, *16*, 054018. [CrossRef]
79. Hirpa, B.A.; Adane, G.B.; Asrat, A.; Nedaw, D.; Song, C.; Roh, M.; Lee, W. Urban Sprawl at the Expense of Cultivated Land: Decadal Land Use and Land Cover Changes and Future Projections in the Upper Awash Basin of Central Ethiopia. *Front. Ecol. Evol.* **2023**, *11*, 1160987. [CrossRef]
80. Hosseini, A.; Mocko, D.M.; Brunsell, N.A.; Kumar, S.V.; Mahanama, S.; Arsenault, K.; Roundy, J.K. Understanding the Impact of Vegetation Dynamics on the Water Cycle in the Noah-MP Model. *Front. Water* **2022**, *4*, 925852. [CrossRef]
81. Karimi, P.; Bastiaanssen, W.G.M. Spatial Evapotranspiration, Rainfall and Land Use Data in Water Accounting—Part 1: Review of the Accuracy of the Remote Sensing Data. *Hydrol. Earth Syst. Sci.* **2015**, *19*, 507–532. [CrossRef]
82. Achugbu, I.C.; Olufayo, A.A.; Balogun, I.A.; Dudhia, J.; McAllister, M.; Adefisan, E.A.; Naabil, E. Potential Effects of Land Use Land Cover Change on Streamflow over the Sokoto Rima River Basin. *Heliyon* **2022**, *8*, e09779. [CrossRef]
83. Tadese, M.; Kumar, L.; Koech, R. Long-Term Variability in Potential Evapotranspiration, Water Availability and Drought under Climate Change Scenarios in the Awash River Basin, Ethiopia. *Atmosphere* **2020**, *11*, 883. [CrossRef]
84. Winkler, K.; Fuchs, R.; Rounsevell, M.; Herold, M. Global Land Use Changes Are Four Times Greater than Previously Estimated. *Nat. Commun.* **2021**, *12*, 2501. [CrossRef] [PubMed]
85. Yang, G.; Xue, L.; He, X.; Wang, C.; Long, A. Change in Land Use and Evapotranspiration in the Manas River Basin, China with Long-Term Water-Saving Measures. *Sci. Rep.* **2017**, *7*, 17874. [CrossRef]
86. Mazrooei, A.; Reitz, M.; Wang, D.; Sankarasubramanian, A. Urbanization Impacts on Evapotranspiration Across Various Spatio-Temporal Scales. *Earth's Future* **2021**, *9*, e2021EF002045. [CrossRef]
87. Gebremicael, T.G.; Mohamed, Y.A.; Zaag, P.V.; Hagos, E.Y. Temporal and Spatial Changes of Rainfall and Streamflow in the Upper Tekezē-Atbara River Basin, Ethiopia. *Hydrol. Earth Syst. Sci.* **2017**, *21*, 2127–2142. [CrossRef]
88. Tufa, Z.D.; Goshel, C.C. Evaluation of ENSO Impact on Surface Water Storage of Awash River Basin In Ethiopia. *J. Earth Sci. Clim. Change* **2023**, *14*, 1000683.
89. Assegide, E.; Alamirew, T.; Dile, Y.T.; Bayabil, H. A Synthesis of Surface Water Quality in Awash Basin, Ethiopia. *Front. Water* **2022**, *4*, 782124. [CrossRef]
90. Getahun, Y.S.; Li, M.H.; Pun, I.F. Trend and Change-Point Detection Analyses of Rainfall and Temperature over the Awash River Basin of Ethiopia. *Heliyon* **2021**, *7*, e08024. [CrossRef]
91. Li, D.; Tian, P.; Luo, H.; Hu, T.; Dong, B.; Cui, Y.; Khan, S.; Luo, Y. Impacts of Land Use and Land Cover Changes on Regional Climate in the Lhasa River Basin, Tibetan Plateau. *Sci. Total Environ.* **2020**, *742*, 140570. [CrossRef]
92. de Ávila, Á.V.A.; de Gonçalves, L.G.G.; Souza, V.d.A.; Alves, L.E.R.; Galetti, G.D.; Maske, B.M.; Getirana, A.; Ruhoff, A.; Biudes, M.S.; Machado, N.G.; et al. Assessing the Performance of the South American Land Data Assimilation System Version 2 (SALDAS-2) Energy Balance across Diverse Biomes. *Atmosphere* **2023**, *14*, 959. [CrossRef]
93. Tariq, S.; Zeydan, Ö.; Nawaz, H.; Mehmood, U.; ul-Haq, Z. Impact of Land Use/Land Cover (LULC) Changes on Latent/Sensible Heat Flux and Precipitation over Türkiye. *Theor. Appl. Climatol.* **2023**, *153*, 1237–1256. [CrossRef]
94. Tokuda, D.; Hsu, H.; Dirmeyer, A. Soil Moisture-Latent Heat Flux Coupling in Climate Modeling: Insights and Implications from the Offline Land Model. *J. Hydrometeorol.* **2025**, *26*, 293–308. [CrossRef]
95. Sahoo, S.; Majumder, A.; Swain, S.; Gareema; Pateriya, B.; Al-Ansari, N. Analysis of Decadal Land Use Changes and Its Impacts on Urban Heat Island (UHI) Using Remote Sensing-Based Approach: A Smart City Perspective. *Sustainability* **2022**, *14*, 11892. [CrossRef]
96. Teklebirhan, A.; Dessie, N.; Tesfamichael, G. Groundwater Recharge, Evapotranspiration and Surface Runoff Estimation Using WetSpass Modeling Method in Illala Catchment, Northern Ethiopia. *Momona Ethiop. J. Sci.* **2012**, *4*, 96. [CrossRef]
97. Chelkeba Tumsa, B. The Response of Sensitive LULC Changes to Runoff and Sediment Yield in a Semihumid Urban Watershed of the Upper Awash Subbasin Using the SWAT+ Model, Oromia, Ethiopia. *Appl. Environ. Soil Sci.* **2023**, *2023*, 6856144. [CrossRef]
98. Getu Engida, T.; Nigussie, T.A.; Aneseyee, A.B.; Barnabas, J. Land Use/Land Cover Change Impact on Hydrological Process in the Upper Baro Basin, Ethiopia. *Appl. Environ. Soil Sci.* **2021**, *2021*, 6617541. [CrossRef]
99. Taddese, G.; Sonder, K.; Peden, D. The Water of the Awash River Basin a Future Challenge to Ethiopia. *Concept Commun.* **2019**, *23*, 301–316. [CrossRef]

Disclaimer/Publisher's Note: The statements, opinions and data contained in all publications are solely those of the individual author(s) and contributor(s) and not of MDPI and/or the editor(s). MDPI and/or the editor(s) disclaim responsibility for any injury to people or property resulting from any ideas, methods, instructions or products referred to in the content.